



Distinguishing Algorithm for Gold Deposit Types

Abdelhalim S. Mahmoud^{1,3}, Mansour M. Abdelsamad¹, Ahmed I. Taha¹, Ahmed H. Mansour^{2,3},
Mariam E. Nassif¹, Sara Kh. Abdelfatah¹, Mera M. Saleeb¹, Rabea A. Khaled⁴

¹Geology Department, Faculty of Science, Fayoum University, Egypt

²Geology Department, Faculty of Science, Assiut University, Egypt

³Russian State Geological Prospecting University, Moscow, Russia

⁴Faculty of computer and information technology, National Egyptian E-learning University, Giza, Egypt

Correspondence e-mail: asm07@fayoum.edu.eg

ABSTRACTS

The determination of gold deposit type holds a great economic significance since each gold deposit type displays its own grade and tonnage and consequently requires different exploration and exploitation strategies. The considerable diversity of gold deposits, combined with the distinctive features inherent to each type and the notable overlap among many deposits, renders the accurate classification of these deposits a complex endeavor. To differentiate between these deposit types, we collected geological, mineralogical, and geochemical characteristics, as well as ore-forming parameters, for 12 gold deposit types. A detailed classification scheme is utilized, covering four specific categories of gold deposits, namely orogenic, including greenstone-hosted, banded iron formation-hosted, and turbidite-hosted; reduced intrusion-related deposits; and oxidized intrusion-related gold deposits, which encompass Au-Cu porphyry, Au-skarn, and high-sulfidation epithermal deposits, with a fourth class incorporating other deposit types, such as low-sulfidation epithermal, Carlin-type, and Au-volcanic massive sulfide deposits. The tabulated distinctive characteristics were used to construct a series of decision trees for gold deposit type identification. The distinguishing algorithm is formulated in the form of a Java computer application. Three decision trees are implemented for the purpose of ascertaining the type of gold deposit. If two decision trees yield a consensus on a particular type, the ore type identification is made accordingly. To validate the outcome, the user is prompted to respond to a series of questions pertaining to the identified type, with the accuracy rate of the responses must exceed 90%. Failure to meet this criterion will result in the decision tree being revisited, and the accurate data will need to be re-entered.

ARTICLE INFO

Article History:

Received 07 Dec 2024

Revised 08 Dec 2024

Accepted 30 Dec 2024

Available 31 Dec 2024

Keyword:

Gold deposit classification, Gold exploration, Decision tree, Distinguishing algorithms, Java.

© 2024 Journal of Geology & Exploration

<https://doi.org/10.58227/jge.v3i2.184>

INTRODUCTION

Gold is a unique element in that it may be located across various types of deposits and tectonic environments, unlike elements such as Cr, Ni, Co, V, Pt etc., which are compatible in mafic intrusive rocks, or elements such as Sn, W, Mo, Nb, Ta etc., which are restricted to felsic ones, it can be found in both mafic and felsic rocks. Although it is a rare metal, it is found even in the bodies of animals and plants, sea water, soil, etc. in low concentrations (Eisler, 2004). This paper is concerned with distinguishing between gold types including both major and minor gold deposit types. Each type of mineralization possesses distinct characteristics and specific environments in which it forms. Nevertheless, there remains a lack of agreement regarding the origins of these atypical deposits. Outlining the footprints and key characteristics of well-established gold deposits is useful for two reasons: firstly, it leads to the identification of mineralization types, which is useful for academic research; and secondly, each mineralization type expresses a different relative economic importance. Therefore, it is advisable to concentrate efforts on models that are most likely to produce large deposits or provide suitable mining strategies for small types.

It is essential to determine the distinctive characteristics and footprints of the major and minor types of gold deposits before judging the mineralization type. However, the matter is not so easy, as rapid development in exploration tools and scientific methodologies has widened the boundaries of



Lisensi: cc-by-sa



each gold mineralization type and even recognized new gold mineralization types. For example, the delineation between the orogenic and reduced intrusion-related gold deposit models exhibits considerable ambiguity discussed by many authors (e.g., Robert et al., 2007; Hart and Goldfarb 2005). An example of the recognition of new gold deposits includes the iron oxide copper gold IOCG deposit, which was recognized as a new gold deposit type emerged during the mid-1980s and early 1990s (Skirrow, 2002). Nonetheless, there exists substantial uncertainty about the exact distinction between this type and various other types.

METHODS

Several classification schemes have been suggested for gold deposits. For example, Robert et al. (1997), Poulsen et al. (2000), and Hagemann and Brown (2000) classified gold deposit types into three clans, which either originated by related processes or that are discrete products of significant hydrothermal systems. The scheme included orogenic, reduced intrusion-related (RIR), and oxidized intrusion-related (OIR) gold classes. Furthermore, significant efforts were made to distinguish between similar pairs of gold mineralization, as exemplified by the criteria outlined by Hart and Goldfarb (2005) for distinguishing intrusion-related gold systems from orogenic ones. We adopted a new classification scheme based upon the most accepted models and terminologies used in recent reviews (e.g., Ridely 2013; Robert et al., 2007). The studied categories of gold mineralizations are presented in Figure. 1, along with their corresponding abbreviations, as follows:

- Orogenic gold class (OG)
 1. Turbidite-hosted gold deposits (TURG)
 2. Greenstone-hosted gold deposits (GSG)
 3. BIF-hosted gold deposits (BIFG)
- Reduced Intrusion-related gold deposits (RIRG)
- Oxidized Intrusion-related gold deposits (OIRG)
 1. Cu-Au porphyry deposits (CAP)
 2. Au-skarn deposits (GS)
 3. High sulfidation epithermal gold deposits (HSEG)
- Other gold deposits (OGD)
 1. Low sulfidation epithermal gold deposits (LSEG)
 2. Au-Volcanic Massive Sulfides (Au-VMS)
 3. Carlin-type gold deposits (CTG)
 4. Polymetallic vein-type deposits (PVT)
 5. Iron oxide copper gold deposits (IOCG)
 6. Paleoplacer gold deposits (PPG)

Discrimination among the gold deposits was constructed according to various geological factors, including the type, characteristics, and tectonic setting of the host rock, as well as the geological characteristics of the ore body, mineralogical features, and the parameters of the ore-forming environment that include salinity, temperature, pressure, depth, and stable isotopic signature (Tables 1-4). So as to address the challenge of identifying the type of gold deposits in a contemporary manner leveraging advancements in computer science, a specific procedure was implemented as the following:

1. An adequate classification scheme for gold deposits was established.
2. All possible key characteristics for the studied 12 gold deposits are defined from a large number of sources. The most frequently occurring characteristics and values were adopted and the outliers were avoided.
3. The points of agreement and differences between the studied gold types were studied carefully from a geological perspective in order to be used for ore type identification.
4. Abbreviations have been created for each gold deposit type in order to facilitate their reading.
5. Three different decision trees were created to distinguish between types based on the distinctive characteristics of each type of mineralization.
6. Creating an algorithmic computer application that takes the decision in two steps: the first step represents an algorithm based on the versions of decision trees.

The second step verifies the decision from the first step. In this step, the user is asked multi-choice questions; some of them are mandatory and others can be skipped. For each type of gold deposit, the user's answer must match the saved correct answer in the program.





RESULTS AND DISCUSSION

Review of the studied gold deposits

According to an evaluation of current gold deposit classification knowledge, there are as a minimum 13 internationally recognized types of gold deposits that fall into three classes, in addition to another that combines other minor deposits (Figure. 1). The primary geological and mineralogical characteristics of both the host and ore body, as well as the tectonic setting and ore-forming parameters, are outlined in Tables 1–4. Examination of this data reveals that the geological setting, mineralization characteristics, and hydrothermal alteration patterns are distinctive for nearly each type of deposit. In order to examine these distinguishing features, it is first essential to give a brief definition of each type with its distinctive features, as follows:

1. **Orogenic gold deposit class** include gold deposits, which are instead known as mesothermal gold deposits, lode Au deposits, quartz vein Au deposits, or Au-only deposits (Kerrick, 1993; Groves et al. 1998). As inferred from their nomenclature, they are formed due to compressional to transpressional deformation events of regionally metamorphosed belts at convergent plate margins within accretionary and collisional orogenies (Goldfarb et al., 1991). These events play a crucial role in their formation, in the creation of shear zones and structural pathways with high permeability for the movement of fluids, and in the deposition and accumulation of gold in specific locations (Vearncombe and Zelic, 2015; Groves et al., 1998). Orogenic gold deposits can be differentiated from intrusion-related deposits as they have a non-igneous origin, primarily sourced from metamorphic materials, with noticeable time gaps between intrusion and mineralization (Barley and Groves, 1992; Hart and Goldfarb 2005). They are considered the most crucial form of gold, with more than 75% of the gold mined by humans throughout history belonging to this category (Phillips and Powell, 2010). There are three distinct categories of orogenic gold deposits: greenstone-hosted, banded iron formation (BIF)-hosted, and turbidite-hosted gold deposits (Robert 1997).

1.1. Greenstone-hosted gold deposits are a type of mesothermal orogenic gold deposits, typically the products commonly associated with intricate hydrothermal systems that encompass multiple fluids at different stages of their evolution. These deposits are commonly found at the contacts between Archean greenstone belts and other rock types, which are predominantly hosted by a sequence of interlayered ultramafic and mafic volcanic or volcanoclastic rocks that have been metamorphosed to greenschist and upper amphibolite facies and associated with sedimentary rocks. The gold mineralization occurs as large vein-like structures related to compressional-to-transpressional shear zones (Kwan et al., 2019).

1.2. Turbidite-hosted gold deposits are structurally-controlled high-grade quartz or quartz carbonate vein deposits occurs in shear zones and are hosted by weakly metamorphosed turbidites, which usually contain graphite. The turbidite formation is characterized by the presence of graywacke sandstone, shale, and/or a combination of pyroclastic and epiclastic sediments, which predominantly consist of chemical sediments such as graphitic chert and graphitic schist, along with minor volcanic rocks (Groves et al., 1998).

1.3. Banded iron formation (BIF)-hosted gold deposits are a type of Archean, stratabound, structurally controlled orogenic gold deposits in the form of Fe-rich layers with sulfide replacements and variably-developed quartz-carbonate veins, silicification zones, or as disseminations in BIFs and related mafic (meta-dolerite and meta-basalt) wall rocks (e.g., Andrianjakavah et al., 2007). They possess the potential to form giant mines such as the Canadian Musselwhite and Meadowbank BIF-hosted gold deposits (Castonguay et al., 2015).

2. Reduced intrusion-related gold (RIRG) class typically is found as sheeted, parallel auriferous quartz veins and veinlets that form high-tonnage, low-grade gold deposits at the apical parts of small plutons. They don't form high-grade vein systems like orogenic deposits do. The most characteristic metals that usually make up RIRG deposits are Au, Bi, Te, and W. Characteristically, the host or related intrusions display moderately low primary oxidation states, which classifies them as reduced intrusions and part of the ilmenite series granitoids (Ishihara, 1981). The granitoid intrusions that give rise to these deposits are formed subsequently as post-collisional intrusions, which are geochemically reduced, alkaline, and rich in volatiles (Hart, 2007). Their primary magmas have no definite source but possess characteristics of S-, I-, and A-type granitoids. The reduced state of the intrusive body responsible for these deposits leads to the prevalence of pyrrhotite over pyrite among the associated sulfide mineral



Typically, reduced intrusion-related deposits originate from magmatic fluids characterized by low salinity at depths ranging from approximately 4 to 6 km. RIRG systems are located far from tectonic plate intersections, instead occurring in continental margin settings that are primarily composed of older, potentially metamorphosed sediments.

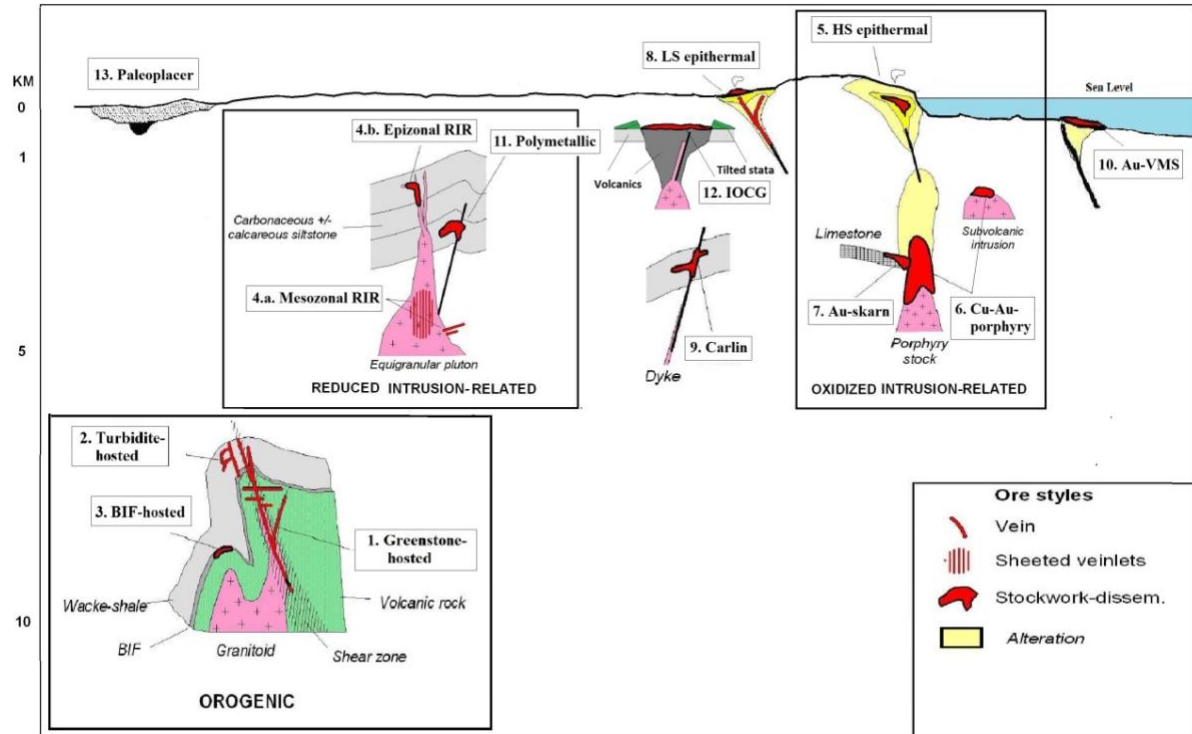


Figure. 1. Schematic cross section illustrating the major and minor gold types and the inferred crustal depths of their deposition after Robert et al., 2007 and Poulsen et al. (2000).

3. Oxidized intrusion-related gold (OICG) class includes the well-known high-sulfidation epithermal deposits, Au-Cu-porphyry, and Au-rich skarn. Generally, they originate in oceanic and continental convergent plate environments. It has been proposed that the most significant deposits of this type are formed within compressional arcs (Hart, 2005). The OIRG systems are most appropriately understood as parts of extensive hydrothermal systems that are predominantly associated with oxidized, shallow, calc-alkaline, intermediate-to-felsic porphyritic copper-bearing stocks situated within magmatic arcs (Robert et al., 2007). The defining characteristics and geological contexts of the alkaline end members of porphyritic deposits have been further delineated, alongside their potential association with low-sulfidation alkali epithermal systems (Jensen and Barton, 2000). Gold is found within a stockwork quartz veinlets hosted by diorite, tonalite, or dacite porphyry, typically located in the core or on the flanks of stratovolcanoes or volcanic dome-vent complexes, which foster long-lived igneous systems. If a significant volume of the overlying volcanic material remains intact, the system may manifest as a high-sulfidation epithermal system characterized by veins exhibiting advanced argillic alteration and vuggy silica replacement.

3.1. Porphyry copper-gold deposits: Copper porphyry deposits can be defined as disseminated copper mineralizations and steeply inclined quartz stockwork bodies centered on igneous felsic or intermediate stocks of sub-volcanic character, typically exhibiting a porphyritic texture (Hewitt et al., 1980; Ridely, 2013). These deposits typically have low-grade ore (average of 0.5 wt.% Cu) mineralization but large tonnage, ranging between 1 Mt and 10 Gt. Gold-rich copper porphyry deposits are identified by having a gold grade exceeding 1 g/t and frequently exhibit a deficiency in molybdenum, in contrast to their elevated concentration of platinum group elements, especially platinum and palladium (Li et al., 2006). The host granitoids vary in composition, ranging from high potassium calc-alkaline quartz monzonite, alkaline monzonite, and syenite to low potassium calc-alkaline diorite, quartz diorite, and tonalite. Six distinct alteration zones are evident in these deposits, encompassing Ca-Na silicate alteration, potassic silicate alteration, propylitic alteration, intermediate argillic alteration, phyllic (sericitic) alteration, and advanced argillic alteration. They commonly originate at shallow crustal levels,



specifically between 1 and 2 kilometers and, hence, exhibit low oxygen fugacity. Predominantly, Cu-Au-porphyry deposits are generated within subduction-related volcanic-plutonic arcs and continental margin arcs that exist at convergent tectonic plate boundaries (Ridely, 2013) and likely associated with hydrothermal breccias and coeval felsic adakitic volcanic rocks that formed from the anatexis of altered basalt associated with subducted oceanic slabs (Li et al., 2006). The majority of these deposits dates back to the Phanerozoic era, with a few exceptions being of Precambrian age (Franklin and Thorpe, 1982).

3.2. Au-Skarn deposits: The term "skarn" that originated in the old mines of Sweden is now commonly employed to describe the assemblages of iron-bearing calc-silicate gangue minerals, such as garnet, diopside, and wollastonite, which are typically found in association with certain sulfide ores. Au-skarn term proposed by Einaudi et al. (1981), is utilized in an economic context to denote specific ore deposits that exhibit calc-silicate alteration. Gold is frequently found as the main commodity or as a notable by-product in various Au-skarn deposits (Orris et al., 1987). In comparison to ordinary porphyry deposits, skarn deposits are noted for their high-grade but lower tonnage. Au-skarn deposits, like other types of skarn, are typically localized due to a confluence of structural and lithological factors. The formation of prograde gangue mineral assemblages within skarn deposits occurs at temperatures approximately estimated to be between 450 to 600 °C (Einaudi et al., 1981). The distributions of skarn and carbonate-replacement deposits around magmatic centers and their forms are variable. Although many Au-skarn deposits are categorized into the reduced intrusion-related gold deposit class (e.g., Meinert, 1992), an increasing number of economically significant Au-skarn deposits have been identified as oxidized intrusion-related gold deposits (e.g., Ettlinger and Meinert 1991; Forster et al. 2004; Fontbote et al. 2005). This study classifies Au-skarn deposits to the oxidized intrusion-related gold deposit class. The preference to relate Au-skarn to oxidized Au-skarn deposits are attributed to their association with Cu-Au-porphyry deposits associated with calc-alkaline and alkaline potassic magmatism (Müller and Groves 1997; Meinert et al. 2005).

3.3. High-sulfidation Epithermal gold deposits: Epithermal gold deposits are high-grade, small-volume accumulations of gold deposits formed in near-surface hydrothermal systems characterized by low temperatures and low pressures (Ridely, 2013). These deposits typically occur in veins or breccia zones and are associated with extensive alteration zones in the surrounding rocks. High-sulfidation (HS) epithermal gold deposits are economically valuable groups of gold and silver that form in deeper, hotter hydrothermal systems with acidic hot springs, a lot of sulfur, and a specific set of ore and gangue minerals. HS epithermal deposits are often found as veins, vuggy breccias, and sulphide replacements associated with various types of volcanic rocks. They are characterized by acid-leached, advanced argillic, siliceous alteration. High-sulfidation (HS) epithermal gold deposits are genetically linked to underlying Cu-Au-porphyry deposits and are found in island arcs, back-arc basins, and continental margins (Taylor, 2007).

4. Other types

4.1. Low-sulfidation epithermal gold deposits are economically valuable accumulations of gold and silver originated in shallow, low-temperature (100 to 300 °C) hydrothermal systems in the form of near-neutral hot springs, low sulfur content (such as pyrite and chalcopyrite), and distinct gangue mineral assemblages, including adularia, sericite, quartz, calcite, and rhodochrosite (Sänger-von Oepen et al., 1990; Ridely 2013; Prihatmoko and Idrus 2020). These deposits are often connected to volcanic activity and are found in island arcs, back-arc basins, and continental margins (Ridely, 2013).

4.2. Carlin-type (CT) gold deposit: This term was originally introduced to characterize gold deposits that are hosted within sedimentary formations in central Nevada subsequent to the revelation of the Carlin mine in the 1960s (Simon et al., 1999; Hofstra and Cline, 2000). These deposits are currently renowned for their large tonnage, despite their low grades of as little as 0.7 g/t Au. Carlin-type deposits represent a category of disseminated gold hosted in sedimentary deposits, wherein gold is predominantly associated with auriferous pyrite. The typical host rock is composed of permeable iron-rich carbonate rock. The sulfidation of the iron content of carbonate results in the formation of arsenian pyrite. The distinguishing features include carbonate dissolution, silicate argillization, mineral sulfidation, and limestone silicification. These deposits typically originate at depths exceeding 2 km, under temperatures between 250° and 150°C, involving slightly acidic fluids with a pH of approximately 5, which are reduced and contain low salinity CO₂-rich fluids, with some CH₄ and H₂S (Hofstra and Cline, 2000; Ridely, 2013). The conceptual frameworks regarding the genesis of Carlin deposits have





changed from being classified as epithermal deposits linked to Tertiary magmatism (Radtke, 1985), then reclassified as deep metamorphic deposits (Kuehn and Rose, 1995), and more recently, as moderate-depth hydrothermal deposits (Hofstra and Cline, 2000; Muntean et al., 2011).

4.3. Au-VMS deposits: Simply, the term VMS refers to a type of mineral deposit consisting predominantly of iron, copper, zinc, and lead sulfides, along with significant concentrations of silver and gold. These deposits originate on or beneath the ocean or sea floor, resulting from the hydrothermal processes associated with submarine volcanic activity. According to the classification established by Poulsen and Hannington (1996), Au-rich volcanic-hosted massive sulfide (VMS) deposits are defined as those exhibiting gold concentrations in parts per million (ppm) that surpass the total weight percentage of the base metals, specifically zinc, copper, and lead. Similar to the majority of VMS deposits, these formations are characterized by semi-massive to massive sulfide lenses that are concordant to the surrounding lithologies, resting upon discordant stockwork feeder zones (Poulsen and Hannington, 1996; Hannington et al., 1997; Huston, 2000; Poulsen et al., 2000).

4.4. Polymetallic vein-type deposits: It is also known as polymetallic replacement deposits, carbonate replacement deposits, and high-temperature carbonate-hosted Ag-Pb-Zn deposits. They represent a large number of small quartz-carbonate veins which contain gold and silver in association with disseminated base metal sulfides or localized accumulations of massive sulfide minerals. These deposits are formed in and around magmatic centers by the replacement of sedimentary rocks, predominantly carbonate in nature, through the infiltration of metal-bearing fluids in areas adjacent to felsic hypabyssal porphyry igneous intrusions along fault zones (Sangster, 1984; Cox, 1986; Ridely, 2013). The width of these ore veins can range from several centimeters to nearly 10 meters, with intervals between them potentially reaching up to one kilometer. Typically, there are one or several sets of veins oriented in a specific direction, with incremental changes in orientation resembling those observed in veinlets found in porphyry deposits. Tin-bearing systems are commonly found and are often linked to equigranular granites that have extensive surface exposure, intruding to depths of a few kilometers in the crust of the Earth (Ridely, 2013). The key aspect is the zoned ore fields of the veins, together with the alteration assemblages located in the vicinity of the veins. The zonal pattern includes wolframite and bismuthinite occur in the central part, followed by cassiterite, arsenopyrite, and chalcopyrite, and sphalerite and galena in the peripheral areas (Ridely, 2013; Maffini et al., 2017).

4.5. Iron oxide copper gold (IOCG) deposits are a relatively newly defined gold and copper deposit type characterized by a high concentration of low-titanium varieties of iron oxide such as magnetite and/or hematite over iron-sulfide minerals like pyrite (Meyer, 1988; Hitzman et al., 1992; Barton and Johnson, 1996; Sillitoe, 2003; Williams et al., 2005; Porter, 2010; Chen, 2013). IOCG deposits are known for their progressive alteration zonation originating from the core: (a) moderately oxidized potassium-iron-rich minerals, including K-feldspar, magnetite, biotite, and amphibole; evolving into (b) highly oxidized potassium-iron-calcium-CO₂-rich minerals like sericite, chlorite, hematite, carbonate, and quartz; and (c) silica-iron-rich vein minerals including hematite and quartz (Richards and Mumin 2013). These deposits occur in association with multiple rock types, such as granite, felsic volcanic/volcaniclastic rocks, and mafic igneous rocks (Skirrow et al., 2019). These deposits exhibit significant structural controls and are temporally associated with magmatic intrusions, although they do not share a close spatial relationship (Williams et al., 2005). IOCG frequently originate in rift or subduction-related tectonic settings (Hitzman, 2000; Barton, 2014) covering an extensive timeframe that extends from the Late Archean era to the Pliocene epoch (Groves et al., 2010). Additionally, they have the potential to generate various metals as by-products and co-products such as uranium, silver, and light rare earth elements. IOCG mineralizations are observed as vein or breccia-type alteration incorporating sulfides, copper, that is typically associated with low-temperature environments (e.g., Hitzman et al. 1992; De Haller and Fontboté 2009; Hayward and Skirrow 2010).

Distinguishing factors

Various gold deposits display distinct characteristics that assist in their recognition. Nevertheless, there are numerous common features that can lead to ambiguity in taking the decision concerning its type. For example, Cu-Au-porphyry deposits and RIR gold deposits exhibit many similarities, such as their association with granitoids, disseminated nature, significant high tonnage, and low grade. The distinction between this pair necessitates considering additional factors such as host rock characteristics (size of intrusion, textures, geochemical affinity, etc.), depth of formation, oxygen fugacity, and stable isotope signature. Therefore, it is imperative to exercise caution, and decisions





must be based on multiple factors. The subsequent section delineates the key features used to differentiate between different gold deposit types.

1. Host rocks characteristics

1.1. Host rock type

The type of the host rock represents the main factor for classifying of most gold deposits. There are many types of host rocks, comprising igneous, metamorphic, and sedimentary rocks. Within the realm of igneous rocks, there exists a considerable assortment of intrusive rocks that display a composition spanning from intermediate to felsic and mafic (amphibolites, diorite, quartz diorite, granodiorite monzonite, quartz monzonite, granodiorite, granite to monzonite, and granodiorite), extrusive rocks, pyroclastic rocks, and BIF. Sedimentary rocks include chemical sediments (carbonates, dolomitic limestones, and chert), clastic sediments (breccias, sandstone, shale, and turbidites), and carbonate-rich clastic rocks (shaly limestones and limey shales). Metamorphic rocks are not common host rocks except in orogenic types, which are hosted mainly by metamorphosed rocks such as meta-igneous and schists (Goldfarb and Pitcairn 2023). Granitoid rocks appear as the most common host for gold deposits, including greenstone-hosted, reduced IR, HS epithermal, Cu-Au porphyry, Au-skarn, and LS epithermal. These granitoid hosts were classified according to oxygen fugacity into deep-seated reduced granitoids and shallow oxidized intrusions (Table 1), which can be deduced from microprobe data. Other gold deposit types are hosted in volcanic rocks include BIF-hosted, LS epithermal, Au-VMS, and IOCG. Some ore deposits are not restricted to a definite host but are found in a wide variety of hosts, such as Cu-Au-porphyry, LS epithermal, and IOCG. Carbonate-bearing host rocks are common in some deposits such as Au-skarn, polymetallic vein-type and Carlin-type gold deposits.

1.2. Characteristic features of the host rock

The characteristic features of the host rock encompass variable factors, including the textures of the host rock, the environment in which the host rock was deposited, the presence of some enriched elements in the host rock, and the geochemical affinity of the host rock. When gold deposits share the same type of host rock, they can still be distinguished based on the specific characteristics of the host rock. For example, RIRG deposits are found in metaluminous, and occasionally peraluminous, calc-alkaline granitoids (Hart, 2007), while Cu-Au-porphyry deposits are located in peraluminous calc-alkaline to quartz-poor alkaline granitoids (Berger et al., 2008). Additionally, RIRG deposits are identified by various host rock textures, such as equigranular, unidirectional solidification textures, replacement textures, metasomatic-relict, exsolution, poikilitic, and cataclastic textures (Thompson and Newberry 2000). The Cu-Au porphyry deposits are distinguished by the porphyritic texture of their host rock (Berger et al., 2008). Also, the original rock textures that appear 'washed out' which are found only in IOCG (Barton et al., 2013). The deposition environment of the host rock can be used to differentiate between Au-VMS and LS epithermal gold deposits. Although Au-VMS and low-sulfidation epithermal deposits share a similar volcanic host and ore mineralogy, Au-VMS is situated in submarine volcanic rocks, while LS epithermal gold deposits are located in sub-aerial volcanic rocks (Hannington and Herzig 1993).

1.3. Tectonic setting

Gold deposits are frequently originate in subduction-related tectonic environments; these include orogenic, reduced IR, HS epithermal, Cu-Au porphyry, Au-skarn, LS epithermal, Au-VMS, polymetallic, and IOCG. Subduction-related tectonic environments encompasses various environments such as oceanic volcanic island arcs, continental island arcs, back-arc basins, and fore-arc basins (Figure. 2). While most gold deposits tend to form in one or more of these settings, some deposits are specific to certain tectonic environments, providing a useful means of differentiation. For example, Carlin-type deposits are associated with post-collisional tectonic settings and incipient extensional regimes (e.g., Muntean et al., 2011); Au-skarn deposits initiate in island arc orogenic belts (e.g., Chen et al., 2007); and LS epithermal deposits occur in active volcanic island arcs (e.g., Prihatmoko and Idrus 2020). Additionally, Au-VMS deposits are primarily linked to mid-ocean ridge (MOR) environments, although they can also develop in island arcs, rifted arcs, back-arc basins, or back-arc rifts (Dusel-Bacon et al., 2007; Ridely, 2013). Other gold deposits form in overprinted or transitional tectonic settings. For example, IOCG deposits form in an orogenic, continental margin magmatic arc setting that was overprinted by multiple orogenic events, two of which were associated with the formation of syn- to late-orogenic deposits (Hunt et al., 2007). Some gold deposits exhibit a wide variety of tectonic environments. For example, RIRG deposits were detected only in back-arc settings that were related to subduction, while others recorded were related to either collision or post-collision settings (e.g.,



Thompson et al., 1999). Other gold deposits form in overprinted tectonic settings or the transition between two tectonic environments; for example, the formation of IOCG deposits occurs in an anorogenic, magmatic arc on the continental margin setting that has experienced several orogenic events, with two of these events being related to the development of syn- to late-orogenic structures (Hunt et al., 2007).

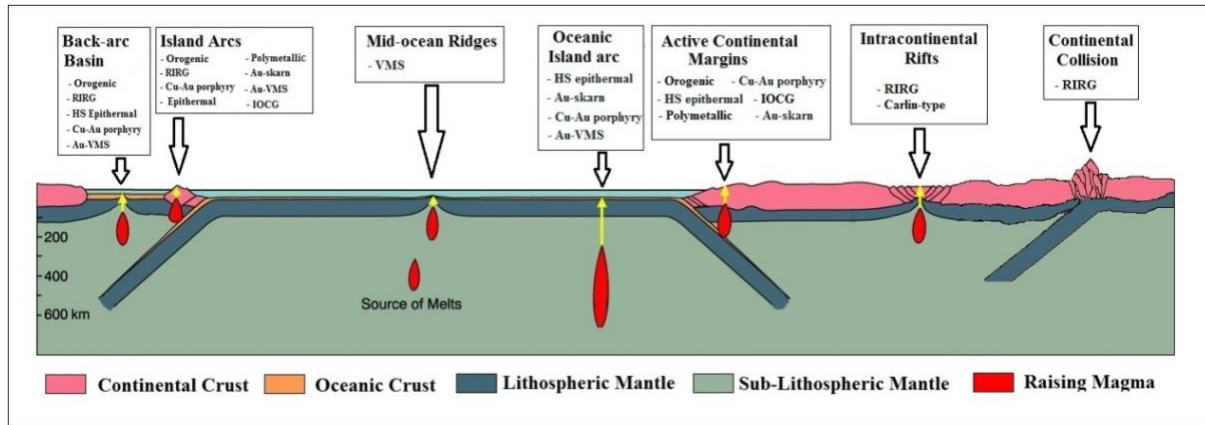


Figure.2. Schematic cross section across the earth's lithosphere showing various tectonic settings and the related gold deposit types.

1.4. Host rock age

The majority of gold deposits are characterized by the Phanerozoic ages of their host rock. However, orogenic gold deposits are unique in that they are restricted to the Precambrian era (Ridely, 2013), serving as a key distinguishing feature for this category. The Phanerozoic age can be linked to the weathering of gold deposits that originated during the Precambrian period, as they were exposed to prolonged erosion. Nonetheless, certain gold deposits are not constrained by specific ages and have the potential to be found across all geological epochs. These include Au-skarn, Au-VMS, polymetallic, and IOCG deposits. For this reason, host rock age is a contributing but not a decisive factor in determining the type of the gold deposit.

2. Geological characteristics of the ore body

2.1. Shape and nature of ore

Gold deposits occur in various shapes and exhibit different natures. The shapes and natures of the investigated gold deposits are thoroughly outlined in Table 2. These two factors are crucial in distinguishing different types of gold deposits. For instance, the ore-bearing veins of the RIRG deposits are famous their sheeted nature which can be also associated with other forms such as massive bodies, banded, disseminated, and brecciated forms (Hart, 2007). Generally, vein-type with stockwork or disseminated sulfide minerals is the main nature of most gold deposits expressed by orogenic, RIRGS, HS epithermal, Cu-Au porphyry, LS epithermal, and polymetallic vein-type. Following this, massive sulfide lenses, such as those found in BIF-hosted orogenic gold, RIRG, Au-VMS, and Au-skarn, come in second-order abundance. These massive sulfide lenses are typically alien to the bedding and may be hosted in local structures. Gold deposits related to magmatic granitic rocks usually exhibit a disseminated, stockwork sulfides embedded in the granite texture or in the associated quartz veinlites. Additionally, some deposits, like IOCG, demonstrate characteristic ore body shapes, such as pipe- to funnel-like structures with extensive hematite-rich breccia-vein sheets within the host stratigraphy (Skirrow, 2022).

2.2. Ore body size/tonnage

The ore body size and tonnage represent the basis for classifying gold deposits into two classes: major gold deposits, including the orogenic ore types, RIRGS, and Cu-Au porphyries with large tonnages greater than 1 MT of ore. Minor gold deposits include Au-skarn, low-sulfidation epithermal, Carlin-type, polymetallic vein-type, and IOCG deposits. Occasionally, rare deposits of the minor class show huge sizes with large tonnages (Table 2). Au-VMS cannot be classified as major or minor as it



usually expresses small to moderate sizes (1-50 MT), but some deposits express huge tonnage, such as the Kidd Crick with more than 138 MT of ores (Barrie et al., 1997).

2.3. Ore grade

Depending solely on ore grade as a definitive factor in differentiating between similar gold deposit types can pose challenges. This difficulty arises from the presence of varying grades within a single ore body in certain deposits, such as those found in HS epithermal deposits where high grades up to 400 g/t related to vuggy silica veins while the lowest grades are in veins related to advanced argillic alteration zones (Ruggieri et al., 1997). Nevertheless, the average ore grade can serve as a useful indicator for differentiation, particularly when there is a significant contrast between ore types, as is the situation with Cu-Au-porphyry and HS epithermal deposits. For example, Cu-Au-porphyry deposits are recognized for their low grade, whereas orogenic and HS epithermal gold deposits are characterized by their high gold grades (Ridely, 2013). Furthermore, high grade are high where the ore is localized in distinct zones, like turbidite-hosted gold deposits, where gold is concentrated at the junction of quartz veins and the surrounding slate host rock (Cox et al., 1995).

2.4. Localization of mineralization

The localization of mineralization is influenced by various factors that govern the deposition of ore minerals. These factors encompass structural components such as faults, shear zones, joints, and the hinge zones of folds, alongside lithological components including bedding planes, foliation, pore spaces, and the contacts between different rock units. The deposition of ore minerals is often a result of the interplay between structural and lithological factors. It is essential to recognize that lithological factors alone are insufficient to dictate the deposition of ore minerals, while structural factors can be effective independently. Structural factors are particularly significant in controlling the deposition of diverse types of gold deposits, whether acting alone, as seen in greenstone-hosted, BIF-hosted, RIRGS, high sulfidation epithermal, low sulfidation epithermal, Cu-Au porphyry, and Carlin-type deposits, or in combination with both structural and lithological factors, as demonstrated in turbidite-hosted, Au-skarn, Au-VMS, polymetallic vein-type, and IOCG deposits. This understanding is crucial for mining geologists in pinpointing the locations of high-grade ores. For example, most Cu-Au porphyry mineralization tends to be concentrated in the apical parts of stocks (Ridely, 2013). Similarly, high-grade gold mineralizations in turbidite-hosted deposits are found predominantly in veins that intersect with carbonaceous slates (Cox et al., 1995).

2.5. Depth of formation

Depth of ore formation represent the basis for classifying intrusion-related gold deposits into oxidized that form at shallow depths and reduced form at greater depths. Determining the depth of mineralization can be achieved through the application of the fluid inclusion geobarometer (e.g., Shelton et al., 2004). The formation of gold ore deposits occurs at different depths, including shallow (< 4 km), moderate (4 to 6 km), and deep (> 6 km up to 10 km). The depth of formation has great influence on various factors such as ore-forming temperature, sulfur and oxygen fugacity, form of sulfur, sulfidation state, and oxygen and sulfur isotopes and consequently on the ore mineralogy and mechanisms for gold precipitation (Zhang et al., 2011; Pokrovski et al., 2015; Keith et al., 2014). It has been noted that the predominant occurrence of gold deposits is at shallow depths (Table 2). However, certain gold deposits, like Carlin-type, exhibit variable depths ranging from 1 to 6 km (Rui-Zhong et al., 2000). Only a few gold deposits are observed to be formed at moderate and deep depths, such as the three orogenic gold types (turbidite-hosted, greenstone-hosted, and BIF-hosted) and the Carlin type. IOCG and Au-skarn deposits do not have a specific depth restriction, but they are typically found at shallow depths.

2.6. Structural regime

The majority of gold deposits are formed in a compressional structural regime, such as orogenic gold types, RIRG, HS epithermal, Cu-Au porphyry, Au-skarn, Carlin-type, and IOCG (Table 2). However, a significant number of these deposits are formed during the transition from compressional regime to extensional one (e.g., Pirajno, 2012; Skirrow, 2022), including Carlin-type, Au-skarn, HS epithermal, and RIRG. Only a small number of gold deposits are exclusively related to extension, such as polymetallic vein-type, LS epithermal, and Au-VMS. Therefore, the structural regime serves as a significant criterion for distinguishing between similar pairs of gold deposit such as Carlin-type and turbidite-hosted, polymetallic vein-type and HS epithermal, and Au-VMS and turbidite-hosted gold deposits.





2.7. Dipping of vein-type deposits

Ore deposits can be classified into stratiform and stratabound based on their situation in conjunction with the bedding of the host rock. Most vein-type gold deposits, including orogenic, RIRG, HS epithermal, LS epithermal, Carlin-type, and polymetallic vein-type, are steeply inclined (Table 2). Some non-veined gold deposits that do not have a definite shape but have disseminated sulfides in the granitic mesh, such as Cu-Au porphyry, have no dip angle. Au-skarn deposits form as disseminations or massive lenses usually parallel to the contact with the source pluton. Usually, this contact zone with the host carbonate is nearly horizontal. The typical Au-VMS ore body is composed of a stratiform sulfide lens and a nearly vertical cone-shaped stringer zone.

3. Ore-mineralogical characteristics

3.1. Ore mineralogy

Gold deposits can be classified into two primary categories based on their mineral composition. The first category includes polymetallic deposits, which consist of HS epithermal, Au-skarn, LS epithermal, Carlin-type, Au-VMS, and polymetallic vein-type deposits. The second category comprises deposits characterized by simpler mineralogical compositions, such as orogenic, RIRG, Cu-Au porphyry, and IOCG deposits. Furthermore, these deposits can also be classified according to the dominant ore minerals, with sulfide-dominant deposits encompassing all types except for BIF-hosted and IOCG deposits, which are classified as oxide-dominated (refer to Table 3). Each type of gold deposit exhibits a distinct mineral composition that distinguishes it from others. Common minerals found in various gold deposits include pyrite, chalcopyrite, and arsenopyrite, with additional minerals like magnetite and hematite specific to BIF and IOCG deposits. Moreover, covellite is unique to epithermal deposits, enargite is characteristic of polymetallic vein-type ores, tetrahedrite is common in HS epithermal, Au-VMS, and polymetallic vein-type deposits, and pyrrhotite is commonly associated with orogenic, RIRG, LS epithermal, polymetallic vein-type, and IOCG deposits.

3.2 . Metal association

The metal associations of various gold deposits represent powerful distinguishing parameters. Table 3 provides a list of the characteristic metal associations for the 12 types of gold deposits under consideration. For example, thallium (Tl) is particularly indicative of Carlin-type gold deposits (Su et al., 2012; Rui-Zhong et al., 2002), while elevated uranium levels are characteristic of IOCG deposits like the Olympic Dam deposit (Corriveau, 2007). Arsenic (As) is associated with specific types of ores, including epithermal, polymetallic vein-type, Au-VMS, Carlin-type, and Au-skarn deposits. Additionally, Hg is characteristic of greenstone-hosted, epithermal, Carlin-type, Au-VMS, and polymetallic vein-type deposits. IOCG, BIF-hosted, and turbidite-hosted gold deposits are distinguished by metal associations rich in Fe. High bismuth (Bi) contents are indicative of deposits such as polymetallic vein type, RIRG, Au-skarn, LS epithermal, Au-VMS, and IOCG deposits. Cu-Au porphyry deposits are commonly characterized by elements such as copper and molybdenum (Ridely, 2013).

3.3. Gangue minerals

Gangue minerals are generally unwanted materials or impurities that are present in the ore. Among the various types of gold deposits, quartz is recognized as the most frequently occurring gangue mineral, with the notable exception of Au-skarn deposits. Adularia (low-temperature feldspar) is a unique gangue mineral that is characteristic for low-sulfidation epithermal deposits (Prihatmoko and Idrus 2020). Barite is usually found in large contents in Au-VMS (Mahmoud et al., 2019). The second most common gangue is sericite, which appears in orogenic, RIRG, and OIRG deposits except Au-skarn. Orogenic gold, Au-skarn, and high-sulfidation epithermal deposits share the high abundance of carbonate gangue, while Au-skarn and high-sulfidation only share the presence of garnet, which may be associated with diopside and wollastonite in Au-skarn. Calcite appears in Carlin-type with serpentine or in polymetallic with fluorite. Fluorite may also be found in epithermal gold deposits (Rhys et al., 2020). K-feldspars appear in many deposits, such as RIRG, HS epithermal, and turbidite-hosted gold deposits. Chlorite appears in Cu-Au porphyry, greenstone-hosted, turbidite-hosted, HS epithermal, and IOCG deposits (which may also contain biotite or actinolite). Greenstone-hosted and HS deposits share some gangue minerals such as amphibole, tourmaline, and biotite, which also appear in Cu-Au porphyry. Cu-Au porphyry may also contain anhydrite, epidote, magnetite, plagioclase, and calcite. In addition to all these gangue minerals, HS epithermal deposits may contain a lot of other gangue minerals.





3.4. Alteration mineralogy

Mineral alteration refers to the natural processes that induce a transformation in the chemical and mineralogical composition or crystallography of the rocks. There are many types of alteration associated with gold deposits, which are essential indicators to discover new ore deposits. Also, recognizing the type of alteration is crucial in mineral exploration as it can offer insights into the hydrothermal system's nature and the potential mineralization type (Mathieu, 2018). The alteration process is subject to various influencing factors, such as the chemical characteristics of the fluid, the conditions of temperature and pressure, the composition of the host rock, and the extent and intensity of the interaction between the fluid and the rock over time (Mathieu, 2018; Pereira et al., 2024).

Sericitization and silicification are the most frequently encountered types of alteration in gold deposits (Table 3). Both of them appear in turbidite-hosted gold and Au-VMS deposits. Sericitization also appears in greenstone-hosted gold and Cu-Au porphyry deposits, where silicification alteration occurs in RIRG, Carlin-type, and epithermal types (HS, LS). Epithermal deposits also have argillic to propylitic alteration. Although low sulfidation epithermal deposits are characterized by sericite-illite/sericite-adularia (phyllitic-argillic) alteration, The RIRG also has an argillic alteration. Chloritization alteration is present in Cu-Au porphyry deposits, while chlorite-sericite alteration occurs in polymetallic veins and chlorite-carbonate in BIF, which may also have sulfidation alteration. There are other types of alteration that are distinct for each deposit, such as carbonatization in greenstone-hosted gold, decalcification in Carlin-type, and aluminous acid alteration causing advanced argillic assemblage in Au-VMS indicates the involvement of an oxidized low-pH hydrothermal fluid (Dubé et al., 2007). IOCG is characterized by sodic and sodic-calcic alteration (Hitzman et al. 1992; Barton and Johnson 1996), while in Au-skarn assemblages, retrograde alteration (high temperatures anhydrous minerals are substituted by hydrous lower temperature minerals) along faults is common (Hammarstrom et al., 1995).

4.5. Ore textures

The identification of certain ore deposits is largely dependent on ore textures, which is a cost-effective method that relies solely on ore section and ore microscope. Although secondary ore textures that are not pertinent to identification may be present, primary textures such as disseminated/stockwork, massive, cavity filling, etc. are significant in this aspect. Disseminated/stockwork texture is the most common texture observed in many gold deposits, such as greenstone-hosted, BIF-hosted, HS epithermal, Cu-Au porphyry, LS epithermal, Carlin-type, and Au-VMS deposits. Certain textures are unique to specific deposit types and are not present in others. For example, the presence of laminated-banded textures that align with the bedding planes of the host clastic rocks is a defining feature of turbidite-hosted orogenic gold deposits (Ramsay et al., 1998). The colloform texture is suggestive of polymetallic vein-type deposits (Cox, 1986), while the euhedrally terminated cavity-filling texture is a distinguishing character of HS epithermal deposits (Dubé et al., 1998). Additionally, the massive and semi-massive textures are associated with Au-skarn and Au-VMS deposits (Ridely, 2013). Ore textures is one of the

4. Ore-forming environment

The identification of ore mineral formation conditions, including the composition and concentration of ore-forming fluids, in addition to the temperature and pressure during ore deposition, is crucial in distinguishing ore deposits. This can be achieved through the investigation of fluid inclusions (FIs), which are commonly abundant in various rocks, minerals, and ores (Randive et al., 2014; Abd El Monsef and Abdelnasser, 2021). Also, stable isotopes such as H, C, O, and S can provide valuable information about the origin of ore-forming fluids and their evolution, in addition to their physical and chemical conditions such as variations in pH, redox conditions, and temperature (Mahmoud et al., 2019; Hutchison et al., 2020; Rui-Zhong et al., 2002).

4.1. Salinity and composition of FIs

The three types of orogenic gold deposits express low salinity but differ in the fluid inclusion composition formed, as the fluid inclusion for greenstone-hosted ore consists of H₂O-CO₂-NaCl; turbidite-hosted ore are CO₂-rich; and BIF-hosted ore consists of H₂O-CO₂±CH₄-NaCl (Table 4). Reduced intrusion-related FIs has two environments, each of which has different salinities from the other, as the shallow environments are an immiscible brine (greater than 30% NaCl equivalent) and low-salinity vapor (less than 5% NaCl equivalent) enriched in CO₂, and the deep environments are CO₂-rich and low-salinity (less than 10% NaCl equivalent) aqueous fluids are found (Baker, 2002). Oxidized intrusion-related gold deposits contain three types that distinguish each one of them by different salinity and fluid inclusion composition: HS epithermal ores show low-salinity fluid inclusions (0.5–5.5% NaCl),



with some occurrences of high-salinity magmatic inclusions (31.5–44.8% NaCl) at high temperatures (390–500 °C), containing over 99 mol.% H₂O and about 0.5 mol.% CO₂ (Ruggieri et al., 1997). Cu-Au porphyry ores are characterized by a complex wide range of fluid salinities that, during their ascent, transform into two principal fluid types, among these is a high-density brine with a salinity exceeding 40 wt.%, which contains chloride salts of Na, K, Fe, Cu, Pb, Zn, and Mn, along with minor CO₂ and substantial concentrations of sulfur-bearing gases such as SO₂ and H₂S. (Klemm et al., 2007; Ulrich et al., 2001; Bodnar and Cline 1991; Bodnar, 1995). Au-skarn deposits exhibit either high salinity (up to 65% NaCl) or moderate-to-low salinity (23–2% NaCl) deduced from fluid inclusions in garnet and epidote (Soloviev et al., 2019). Au-VMS ores have salinities close to seawater values, ranging from 1.4 to 9.6 wt.% NaCl equivalent (Ridely, 2013). The fluid inclusions in Au-VMS are composed of gases such as CO₂, CH₄, N₂, SO₂, and H₂S with numerous cations and anions in Table 4 (Boulanger et al., 2010; Tajeddin et al., 2019). LS Epithermal ores have a salinity ranging from less than 1 to 10 wt.% NaCl equivalent with compositions include aqueous-carbonic liquid-rich inclusions in addition to aqueous-carbonic vapor-rich fluid inclusions (Scott and Watanabe 1998; Angeles et al., 2002). Carlin-type ores exhibit low salinity, about 0 to 7 wt.% NaCl, mostly around 6 wt.% NaCl equivalent. The fluid inclusion composition includes aqueous fluids with low but detectable CO₂ (less than 4 mol%) and H₂S (Hofstra and Cline 2000; Rui-Zhong et al., 2002).

4.2. Ore-forming temperature

Gold ore deposits form at different temperatures, so ore-forming temperature represents a strong factor in distinguishing gold deposit types (Table 4). The ore-forming temperature is influenced by various factors, with the primary determinant being the proximity to magmatic centers. Ore deposits like Cu-Au porphyry, polymetallic vein-type, Au-skarn, and magmatic IOCG deposits are typically found near magmatic centers and consequently exhibit high temperatures (300 to 750 °C). Conversely, deposits located further away from magmatic centers, such as orogenic (greenstone-hosted, turbidite-hosted, and BIF-hosted), high and low sulfidation epithermal, and Carlin-type deposits, tend to originate at lower to moderate temperatures (< 350 °C). Reduced intrusion-related gold deposits exhibit variable behavior in shallow environments with high temperatures of about 600 °C and in deeper environments with low temperatures of around 200 °C (Hart, 2007; Jia et al., 2019). Hydrothermal fluids associated with Au-VMS are released at temperatures between 200 and 400 °C, occurring without the process of boiling (Ridely, 2013; McPhie and Cas 2015). The determination of gold deposit types cannot rely solely on the temperature factor; it is essential to consider other factors outlined in Tables 1-4.

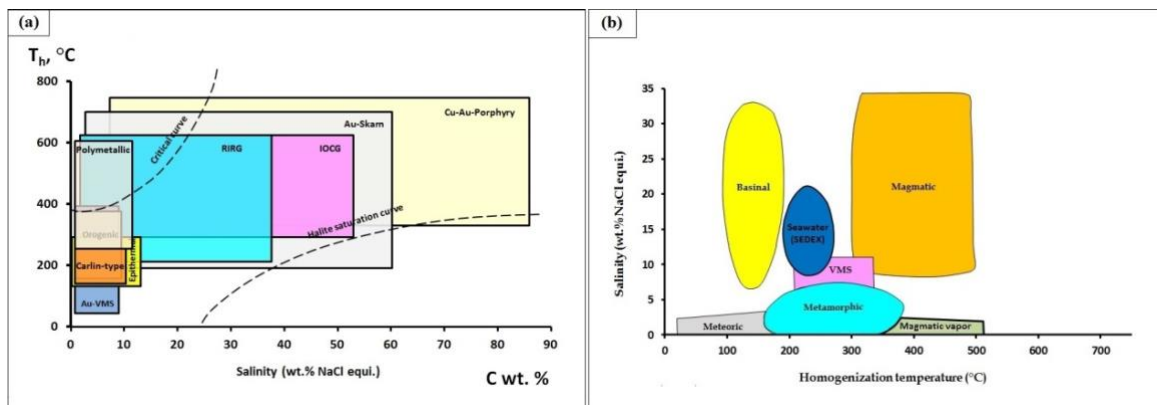


Figure. 3. Classification diagrams of gold deposits constructed based on fluid inclusion data; a) plot of homogenization temperature (°C) vs. salinity (wt.% NaCl equiv.) modified after Wilkinson (2001) to incorporate the targeted gold deposits; (b) plot of salinity vs. homogenization temperature (°C) with reference to fluid inclusions after Kesler (2005).

Various efforts have been made to ascertain the source of fluids. Wilkinson (2001) introduced a diagram that utilizes homogenization temperature versus salinity to discriminate between distinct types of ore deposits. We made modifications to Wilkinson's diagram to include the gold deposits under investigation (Figure. 3a). This diagram is valuable in distinguishing deposits with high salinity and high homogenization temperature, such as Cu-Au porphyry, RIRG, Au-skarn, and magmatic IOCG deposits. Additionally, it can be used to differentiate other low-temperature such as Au-VMS deposits. However, there is significant overlap between most low-temperature and low-salinity deposits, including orogenic,



epithermal, polymetallic vein-type, Carlin-type, and Au-VMS (Figure. 3a). Kesler (2005) also utilized homogenization temperature versus salinity to identify the origin of ore-forming fluids (Figure. 3b). Understanding the origin of ore-forming fluids is crucial in determining the type of gold deposit. For example, the metamorphic source of ore fluids can indicate an orogenic gold deposit type (Abu-Alam et al. 2018).

4.3. Pressure

Gold ore deposits display significant variability in formation pressures. Various factors influence the ore-forming pressure, where the depth of formation and tectonic regime being the primary determinants. It is well-established that depth is directly correlated with pressure. However, while the host rock of the mineralization may be emplaced at significant depths, certain sulfide mineralizations can still form at shallower depths, leading to variable pressure, as observed in RIRG deposits (Baker, 2002). Ore deposits like epithermal (HS and LS), Au-VMS, and polymetallic vein-type deposits typically form near the surface and consequently exhibit low (< 0.5 kbar) pressure (Table 4). Conversely, deposits that originate at great depths (> 5 km), such as orogenic (greenstone-hosted, turbidite-hosted, and BIF-hosted), RIRG, Cu-Au-porphyry, and IOCG, tend to form at high to moderate pressures (0.5 up to 3.5 kbar). Tectonic regime of ore formation also shows a significant role in the pressure as deposits form at compressional tectonic regimes such as orogenic, RIRG, and Cu-Au-porphyry deposits usually express higher pressure than those form at extensional regime. Au-skarn deposits are not restricted to definite depth but usually originates at low depths around 0.5 km, but high pressures between 1 to 3 kbar (Soloviev et al., 2013, 2019). The utilization of pressure as a sole factor in determining the nature of gold deposit is deemed challenging; hence, it is imperative to integrate this parameter with other variables outlined in Tables 1-4.

4.4. Sulfur isotopes and source of fluids

Sulfur isotopic composition is known to deliver important perspectives into the origin of ore-forming fluids and their evolution, in addition to their physical and chemical conditions such as variations in pH, redox conditions, and temperature (Hutchison et al., 2020). Nevertheless, it is often hard to determine which of these processes is the primary driver of isotopic variability. Sulfur isotopes have demonstrated significant efficacy in the exploration of Earth's metallic resources due to the fact that many ore deposits are formed from sulfur- and metal-rich fluids that circulate in the vicinity of magmatic intrusions (Seal, 2006). Given that the majority of economically significant metals have an affinity for sulfur, reduced sulfur plays a crucial role in facilitating the complexation and transport of these metals, especially gold (Mountain and Seward, 2003; Stefánsson and Seward, 2004; Pokrovski et al., 2015), and may also influence their precipitation as stable sulfide minerals. Therefore, the mobility of metals in ore-forming environments is closely tied to the species of sulfur that is reflected in the isotopic composition of minerals containing sulfur (Ohmoto, 1972; Rye, 2005; Seal, 2006).

Gold deposits originating from hydrothermal-magmatic sources, including Cu-Au-porphyry, HS, and LS epithermal gold deposits, in addition to magmatic IOCG, typically exhibit sulfur isotopic values clustering near zero, ranging from -5 to +5‰ (Hutchison et al., 2020). In contrast, deposits such as Au-VMS and Carlin-type demonstrate $\delta^{34}\text{S}$ values with a positive mean (Figure. 4a). Within the orogenic class, greenstone-hosted and BIF-hosted deposits can be differentiated based on their $\delta^{34}\text{S}$ values, with the former displaying a positive mean (Shelton et al., 2004) and the latter showing a negative mean (Bühn et al 2012). Also, $\delta^{34}\text{S}$ is a valuable tool for distinguishing between alteration zones in Au-skarn and LS epithermal deposits (Table 4). HS epithermal and RIRG deposits cannot be distinguished from each other based on sulfur isotopes, as both of them express very similar $\delta^{34}\text{S}$ from -3 to 0 ‰. Some interruption is due to the addition of sulfur isotopes from external sources, comparable to IOCG and Carlin-type gold deposits, such as sulfur contamination from sedimentary or organic sources.

4.5. Oxygen isotopes

Oxygen isotopes have the potential to offer insights into various aspects such as the formation temperature of minerals, the origin of the aqueous fluid, the water to rock ratios, and the degree of chemical equilibrium (Nesbitt, 1996; Campbell and Larson, 1998). A negative value indicates a higher abundance of the lighter isotope, whereas positive values signify a greater content of the heavier isotope. This study specifically delves into the utilization of oxygen isotope anomalies $\delta^{18}\text{O}$ of veined quartz (Table 4), both positive and negative, to distinguish between similar gold deposits. Given that the majority of gold deposits exhibit positive values, our research has been directed towards identifying negative anomalies and exceptionally high or low positive values. LS epithermal, BIF-hosted, and Au-skarn deposits exhibit the lowest values, typically below and around +10‰. Meanwhile, greenstone-





hosted and polymetallic vein-type gold deposits demonstrate an intermediate value ranging between +10 and +15‰. On the other hand, HS epithermal, Au-VMS, turbidite-hosted, and RIRG deposits express the highest values, exceeding +15 ‰ (Figure. 4b). Carlin-type deposits display a broad spectrum of oxygen isotopes in quartz, attributable to the formation of multiple generations of quartz (Yan et al., 2020). It is advisable to consider oxygen isotope values between two pairs when there is a significant difference between them, as illustrated in the ore-forming parameters decision tree (Figure. 7). Also, $\delta^{18}\text{O}$ is a valuable tool for distinguishing between alteration zones in Cu-Au-porphyry deposits and mineralization stages in Au-skarn deposits. However, when $\delta^{18}\text{O}$ of magnetite from BIF-hosted and IOCG deposits, the $\delta^{18}\text{O}$ values are so alike that they are not useful for differentiation.

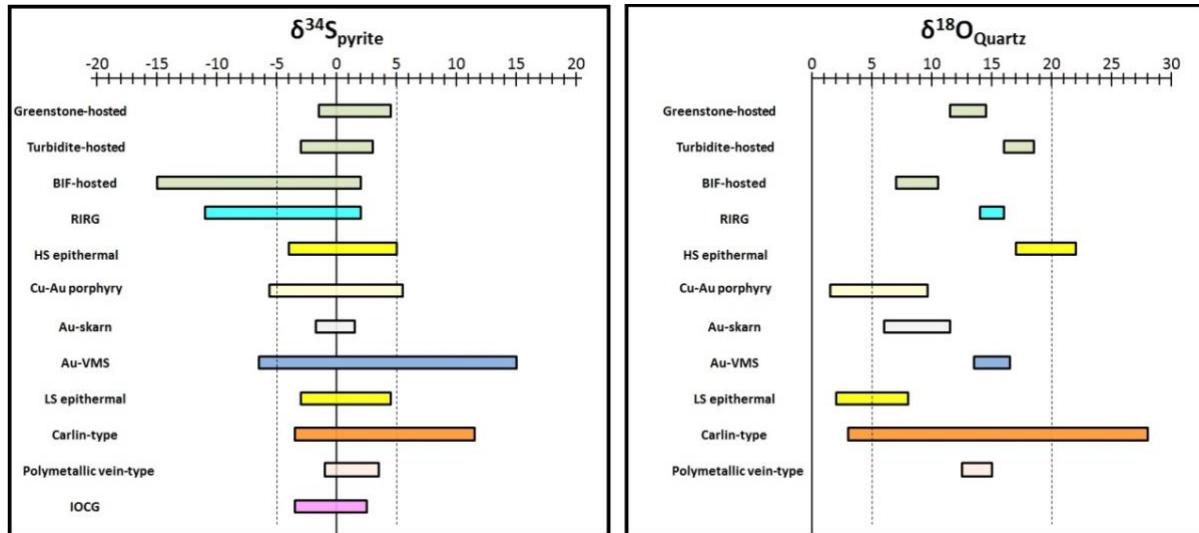


Figure. 4. Sulfur and oxygen isotopic compositions in pyrite and quartz, respectively for different gold deposit types based on data from table 4.

5. Results

The general characters shared by most gold deposits and the distinctive features of each deposit can be outlined as follows:

1. Granitoid and volcanogenic rocks appear as the most common hosts for gold deposits; few deposits are hosted in carbonate rocks; others aren't restricted to a definite host. The mineralogical and geochemical characteristics of the host rock can be used to distinguish between similar gold deposits.
2. Active subduction-related tectonic settings and compressional structural regimes appear to be the most relevant for most gold deposits, although important gold deposits form in anorogenic extensional settings such as Carlin-type.
3. The studied gold deposit types express numerous shapes and ore body natures, which play a significant role in differentiating among them.
4. The size and tonnage of the ore body are fundamental factors used to categorize gold deposits into major and minor types.
5. The majority of gold deposits have Phanerozoic ages, while Precambrian deposits are either poorly preserved or washed out.
6. The majority of gold deposits are structurally regulated, either independently or in conjunction with lithological causes.
7. Gold deposits originate at varying depths, with the bulk occurring at shallow depths (<4 km).
8. The predominant occurrence of vein-type gold deposits is associated with faults that exhibit a steep dip.
9. Pyrite, chalcopyrite, and arsenopyrite are the most common minerals in most gold deposit types. Some minerals are characteristic of some deposits; for example, magnetite and hematite are characteristic of BIF-hosted and IOCG deposits, covellite for epithermal deposits, and enargite for polymetallic vein-type deposits.
10. Each gold deposit has a characteristic metal assemblage that can be used to differentiate between similar types. For example, metal associations with Mo and W are characteristic for Cu-Au-porphyry deposits; Bi, W, Mo, Sb, and Te are characteristic for RIRG; Tl and Se for HS epithermal





- deposits; Te, Se, Cd for Au-skarn; Bi, Te, and Sn for LS epithermal; Sb, Hg, Tl for Carlin-type; Hg, Se, and Bi for Au-VMS; Bi, Te, Hg for Polymetallic vein-type; and Bi and Te for IOCG.
11. Many gangue minerals can be mixed with gold ore, depending on the host rock type and the degree of metasomatism and hydrothermal alteration. The most common of these minerals include, in descending order, quartz, sericite, calcite, chlorite, plagioclase, K-feldspars, biotite, amphibole, and epidote. Some gangue minerals are characteristic for special types of ore; for example, adularia is characteristic for LS epithermal deposits, anhydrite and epidote for Au-Cu-porphyry, and garnet, diopside, and wollastonite for Au-skarn deposits.
 12. Silicification, sericitization, and chloritization are the most common types of alteration in furthestmost gold deposits. Some alteration types are distinct for each deposit, such as carbonatization in greenstone-hosted gold, decalcification in Carlin-type, and aluminous acid (advance argillic) alteration in Au-VMS.
 13. Disseminated stockwork is the most frequently encountered ore texture type nearly all gold deposits. Few gold deposit types, such as Au-VMS, Au-skarn, polymetallic vein-type, and IOCG, are characterized by massive to semi-massive. Some distinct ore textures include colloform textures that distinguish the polymetallic vein-type; and cavity-filling textures that distinguish epithermal deposits.
 14. Most gold deposits, including orogenic gold class, Au-VMS, LS epithermal, and Carlin-type, are formed from low-salinity fluids but different fluid compositions. Reduced intrusions show variable salinities according to depth, where deep ones exhibit moderate salinity while deeply forming ones show low salinity. Also, HS epithermal deposits show variable salinities but are usually low in salinity. Cu-Au porphyry expresses moderate salinity in the peripheral parts, while the core of the deposit is formed from highly saline fluids. Au-skarn deposits exhibit usually high salinity fluids.
 15. Most fluid inclusions illustrate the CO₂-rich nature of most gold deposits, including orogenic, RIRG, and HS epithermal, composed of nearly aqueous fluids. Cu-Au porphyry produces highly saline brine metal chloride salts. Au-VMS shows fluid inclusions of variable constituents, including CO₂, CH₄, N₂, SO₂, and H₂. LS epithermal exhibits an aqueous-carbonic composition. Carlin-type have fluid inclusion with few CO₂ and H₂S.
 16. Ore-forming temperature represents a key factor for distinguishing between many gold deposits; however, it should be combined with other factors such as salinity, tectonic setting, metal association, etc. However, most gold deposits in Carlin are formed at temperatures less than 350 °C, including orogenic gold class, RIRG, and epithermal deposits. Cu-Au-porphyry, polymetallic vein type, and IOCG exhibit temperature zonation, with central parts having a high temperature while peripheral parts are formed at a low temperature. Au-skarn and Au-VMS form at moderate to high temperatures.
 17. Most gold deposits, such as VMS, LS epithermal, and polymetallic vein-type, form at low pressures less than 0.5 kbar. Orogenic gold deposits form at high pressures ranging from 0.5 up to 2.5 kbar, although some BIF-hosted gold deposits can form at pressures around 0.5 kbar. Reduced intrusion-related forms at variable pressure around 1.3 kbar according to the depth of emplacement of magmatic intrusions. Also, IOCG forms at variable pressures of 1.5–3.5 kbar according to their type. Carlin-type is characterized by a high pressure of formation (2.3–4 kbar).
 18. Most gold deposits show $\delta^{34}\text{S}$ for sulfide minerals around zero, with a greater tendency to positive anomalies for greenstone-hosted, Au-VMS, Carlin-type, and polymetallic vein-type deposits. More negative $\delta^{34}\text{S}$ anomalies are expressed by BIF-hosted, RIRG, HS epithermal, and IOCG deposits.
 19. Most gold deposits show positive $\delta^{18}\text{O}_{\text{quartz}}$ values, except for some altered assemblages of Cu-Au-porphyry deposits. The lowest values are expressed by LS epithermal, BIF-hosted, and Au-skarn deposits. Meanwhile, greenstone-hosted and polymetallic vein-type gold deposits demonstrate intermediate values, and HS epithermal, Au-VMS, turbidite-hosted, and RIRG deposits express the highest values.

6. Decision trees

Apart from the decision tree formulated by Robert et al. (1997), which relies on factors such as geological setting, host rock, mineralization form, and geochemical signature, there have been no prior decision trees developed for distinguishing gold deposit types. Nevertheless, the accuracy of their model in identifying gold deposit type is impeded by the potential overlap of parameters. This investigation introduces a computerized methodology that integrates a wider range of variable parameters. The decision-making process involves the utilization of three separate decision trees, followed by validation questions to confirm the determined gold deposit type.





The given decision trees (Figure. 5-7) affirms the problem of geological diversity observed in gold deposits. Gold deposits can be grouped in terms of many factors, including their genesis (i.e., the process responsible for their formation), host rock, localization, inferred depth at which the gold was deposited, tectonic environment, etc. (see tables 1-4 and Figureures 1-3). The genetic classification is the best because it includes such factors as fluid composition, salinity, temperature, pressure, and oxygen fugacity of ore-forming fluids. However, some deposits are thought to be genetically related, and hence distinguishing among them is difficult. For example, HS epithermal gold deposits are the subaerial equivalent of submarine gold-rich volcanic massive sulfide deposits (Hannington and Herzig 1993; Sillitoe et al., 1996; Hannington et al., 1999). Similarly, epithermal gold deposits merge into the intrusion-related class and commonly occur in similar tectonic environments (Robert et al., 1997). Thus, terms like "orogenic," "BIF-hosted gold," "epithermal," and "reduced intrusion-related" all have meaning since they refer to a set of genetically related deposit types that indicate processes responsible for formation, a specific host rock, temperature of formation, and crustal level of gold deposition, respectively. This points to the close association between most gold deposit types and environments.

The complexity of constructing the decision tree stems from the presence of specific deposit types in similar or transnational settings. For example, Cu-Au-porphyry and Au-skarn deposits have been found in both subaerial continental arc and submarine island arc environments. This issue can be resolved by identifying more contrasting and distinguishing parameters. Conversely, some deposits are easily identifiable in the field; for example, IOCG and BIF-hosted deposits can be recognized by their iron-formation host, while the Cu-Au-porphyry deposits are recognized not only by their characteristic host rock as well as by the disseminated habit of mineralization and the hydrothermal alteration zonation. Conversely, gold deposit pairs like RIRG and HS epithermal deposits require additional distinguishing factors, such as the ore-forming pressure determined through fluid inclusion analysis (Figure. 7) or their stable isotope composition.

Many versions of the decision tree can be proposed based on the data in tables 1–4, and many other additional parameters can be added. We used the least expensive parameters to differentiate between similar deposits. Classifications of gold deposits based solely on specific metal associations may contradict those based on geological parameters. For this reason, our decision tree gives priority to geological parameters. These simple observable geological parameters, like the nature of the host rock and the type of mineralization, can greatly reduce the range of potential options and assist an observer in locating evidence of these features, ultimately resulting in more refined distinctions. However, very similar gold deposit types, such as RIR, Cu-Au porphyry, and orogenic gold deposits, need some specific parameters and detailed studies that cost the observer more money, such as the tectonic setting of the host rock and fluid inclusions. Furthermore, it is not always essential to follow the decision trees (Figure. 5-7) from the leftmost side to the rightmost side. As indicated earlier, specific deposits, such as those of the low sulfidation epithermal type, are predominantly identified through a singular parameter, the hydrothermal alteration pattern. This diminishes the necessity to evaluate all additional parameters.

The decision pathways depicted in Figureures 4, 5, and 6 represent some examples of numerous alternative options using only small portion of the available parameters. It is entirely permissible to include additional pathways that could result in new types of deposits or unique individual deposits. Furthermore, it is widely acknowledged that certain deposits can be categorized as belonging to multiple types, as the concept of transitional deposit types, which occur in the zones between porphyry and epithermal environments, has been articulated by several authors in the literature (e.g., Panteleyev, 1996).

In the principal decision tree (Figure. 5), the first step is to observe fundamental parameters such as the host rock type and mineralization form, which can greatly reduce the range of possibilities and guide the observer in identifying indicators of these parameters, facilitating further differentiation. On this basis, host rocks are classified into four types: granitoids, volcanic, pyroclastic, and sedimentary rocks. Note that the same gold deposit may occur in different rock types. The second step can also rely on simple characteristics such as host rock characteristics or mineralization form. The third step can depend on mineralogical characteristics and metal association, which can be determined petrographically or by the chemical analyses of ore minerals. The further parameters need more specific parameters, such as those deduced from fluid inclusion study or isotope analyses.

It is recommended that, after identifying the deposit type for a specific mineralization using the provided decision tree, compare its properties to the typical characteristics of this type from Tables 1-4. If the typical characteristics correlate with the studied deposit by more than 90%, it indicates that the decision tree gives a perfect result. If the typical characteristics don't match the result from the decision tree, it is recommended to check the nearest mineralization type.





7. Implementation steps for decision trees in Java

In this study, we utilized a decision tree approach to classify gold deposits based on various geological parameters. The decision tree algorithm is considered to be one of the most straightforward methods to comprehend and apply. Interestingly, many individuals may have unknowingly utilized this technique for quite some time in their daily decision-making processes, even without being aware of its formal definition. The decision tree implemented in Java is designed to categorize types of gold deposits by prompting the user to input specific geological, mineralogical, geochemical, and environmental condition related to ore formation. The methodology is inherently flexible, allowing for the incorporation of further classification criteria in subsequent iterations. It effectively integrates computational techniques with geological expertise, thereby providing a powerful tool for gold deposits exploration. The program guides users through a sequence of logical questions to determine the deposit type.

7.1. User prompt for tree selection

Upon launching the Java environment and compiling the Gold Deposit program, users will engage with decision trees. The program initiates by prompting the user to select a decision tree type that aligns with their geological interests. The constructed code for this step is shown in (Figure. 8a).

1. Decision tree 1: based on mixed parameters
2. Decision tree 2: based on ore body characteristics
3. Decision tree 3: based on ore-forming environment parameters

After entering the number corresponding to the desired decision tree, the user will be asked a series of questions according to the selected decision trees (Figures. 5-7).

7.2. Decision tree 1 – based on mixed parameters

If the user selects the first tree, he is further asked to specify the type of host rock which is a critical determinant in gold deposit formation. The five categories form the first level of the decision tree as the following (Figure. 8b):

1. Mafic to intermediate intrusions
2. Granitoids
3. Volcanic rocks
4. Pyroclastic rocks
5. Sedimentary rocks

Depending on the choice, the tree navigates through a series of questions about ore minerals, fluid inclusions, ore-forming temperatures, and pressures to classify the deposit. Each specific choice leads to more detailed questions, handled by dedicated methods. The program will then classify the gold deposit type based on user responses. These methods contain nested switch-case statements that further classify the deposit based on more detailed parameters.

7.3. Decision tree 2 – based on ore body characteristics

For the second tree, the user is queried about the main nature of the ore body (Figure. 8c):

1. Vein-dominated
2. Non-veined

Depending on the choice, the tree navigates through a series of questions about vein characteristics, mineral compositions, and ore textures. The program will classify the ore deposit type based on user responses.

7.4. Decision tree 3 – based on ore-forming environment parameters

For the third tree, the user provides details on the ore-forming parameters deduced from the fluid inclusion study and stable isotopes. Firstly, user will be prompted to provide information about the key components that make up the fluid inclusions (Figure. 8d):

1. Mainly aqueous carbonic
2. Mainly aqueous
3. Rich in carbon dioxide
4. Rich in cations
5. Rich in sulfur-bearing gases

Depending on user choice, the subsequent questions about fluid inclusions FIs composition, salinity, temperature, pressure and stable isotopes signature. The program will classify the ore deposit type based on user responses. After each decision tree, the program will ask if you want to try again or choose another decision tree. Entering `1` to try again or `2` to exit and select another decision tree.





Table 1. Type, characteristics and tectonic setting of the host rocks for studied gold deposit types.

Type	Subtype	Host rock types	Characteristic features of the host rock	Tectonic setting	Host rock age	Selected references
A-Orogenic	1- Greenstone-hosted	Metamorphic rocks (sedimentary-volcanic, metavolcanic, metasedimentary rock invaded by granitic intrusions) and mafic igneous rocks such as amphibolites, rarely granitoid host	Regionally metamorphosed to the greenschist facies.	Products of subduction-related tectonics.	Archean	Ridely 2013; Maepa and Smith 2020
	2- Turbidite-hosted	Sandstone (graywackes) and shale or pyroclastic and epiclastic materials, with significant contributions from chemical sediments such as graphitic chert, alongside minor amounts of lava.	Deformed and metamorphosed, Mn-rich sediments, graphite rich.		All ages, mainly Archean	Leube et al., 1990; Berge 2011; Boucher et al., 2015
	3- BIF-hosted	BIF and volcanoclastic successions spatially associated felsic magmas	Polydeformed and metamorphosed up to amphibolite facies.		Precambrian	Sawkins 1972; Castonguay et al., 2015
B- RIRGS	4- Reduced IR	Granitic, granodioritic and monzonitic compositions.	Felsic, mainly predominantly metaluminous, locally peraluminous, calc-alkaline, moderately fractionated, reduced, ilmenite-series granitoids with accessory muscovite, tourmaline, and garnet. Equigranular, unidirectional solidification, metasomatic-relict, replacement, exsolution, poikilitic, and cataclastic textures.	Variable tectonic settings within orogenic belts encompass back-arc regions, foreland fold belts, both collisional and post-collisional settings, and magmatic arc formations.	Phanerozoic	Ishihara, 1981; Hart 2007; Goldfarb et al., 2000; Thompson and Newberry 2000
C- OIRGS	5- HS Epithermal	Extrusive to high-level intrusive rocks with rare pyroclastic rocks	Highly altered intermediate to felsic.	Continental volcanic arcs; intra-oceanic volcanic island arcs; continental back-arc regions.	Phanerozoic (mostly Cenozoic)	Ridely, 2013
	6- Cu-Au porphyry	Diverse rock types of intermediate to felsic composition (SiO ₂ = 52 to 77 wt. %) including diorite, quartz diorite, granodiorite intrusions monzonite, quartz monzonite, or granodiorite rocks.	At least one intrusion have a distinctly porphyritic texture; calc-alkaline; weakly peraluminous; some associated with calc-alkaline to quartz-poor alkaline granitoids. small-volume intrusions	Arc magma (mainly continental arcs; volcanic arc; back-arc) rarely intra-ocean island arcs	Archean to the present; mostly upper Jurassic	Titley, 1982; Ulrich and Heinrich, 2002; Proffett, 2003; Harris et al., 2005; Khashgerel et al., 2006
	7- Au-skarn	Hosted in carbonates, associated with relatively mafic diorite and granodiorite plutons.	Carbonates usually contain a significant clastic or volcanoclastic component	Island arc orogenic belt	Phanerozoic (mostly Cenozoic and Mesozoic)	Meinert 1998; Wu and Kainan 2016
D- Other types	8- LS Epithermal	A greater variety of rock types including sub-aerial volcanic rocks; Typical host sequence is composed of stratified lava deposits and pyroclastic rocks.	Intermediate to felsic composition volcanic rocks	Active volcanic island arcs	Phanerozoic (mostly Cenozoic)	White et al 1995; Ridely, 2013
	9- Carlin-type	Wide Variety, but most commonly hosted in limey shales and shaly limestones, and less frequently encountered impure dolomitic limestones.	Related to calc-alkaline, intermediate to felsic magmatism	Post-collisional and incipient extensional tectonic settings	Phanerozoic (mostly Mid-Tertiary)	Maryono 1998; Ridely, 2013
	10- Au-VMS	Submarine volcanic rocks along with various deep-sea sedimentary rocks; less frequently encountered in turbidites	Bimodal volcanics: mafic to felsic and bimodal siliciclastic in greenstone belts	Adjacent to mid-ocean ridges (MORs), island arcs, rifted arcs, back-arc basins or back-arc rifts.	All ages (Archean to recent)	Hannington et al., 1997; Huston, 2000; Dubé, et al. 2007; Ridely, 2013; Mahmoud et al., 2021
	11- Polymetallic vein-type	the most common host is carbonate-rich sedimentary rocks such as limestone, dolomite, sandstone, and shale intruded by stocks, dikes, and sills of intermediate to felsic composition.	Carbonates rich in Zn and Pb	Continental margin and island arc volcanic-plutonic belts.	All ages (mostly Mesozoic and Cenozoic)	Morris and Cox 1986; Norton, 1989
	12- IOCG	Not restricted to particular host rock type; most commonly in breccias and may be hosted in ironstone, mafic to felsic intrusions, volcanic, and sedimentary rocks.	Some deposits show brecciation, coupled with widespread K and Fe metasomatism evidenced by the significant presence of K-feldspar, chlorite, and hematite. This alteration has resulted in the original textures of the host rock appearing washed out.	Various anorogenic, syn-orogenic and post-orogenic tectonic settings comprising magmatic arcs and continental margin, overprinted by several orogenic events	All ages	Knutson et al., 1979; Hunt et al., 2007





Table 2. Geological characteristics of ore body of the studied gold types.

Ore type	Shape and nature of ore	Deposit size or tonnage	Grade	Localization of mineralization	Depth of formation	Structural regime	Ore body dipping (Angle)	References	
A-Orogenic	1-Greenstone-hosted	Quartz-carbonate veins with disseminated-stockwork-crustiform sulfides combined with brittle-ductile shear zones	Typically, the sizes vary significantly, with some being large while others are relatively small, measuring less than or around 1 MT.	High-grade (average 10 g/t Au)	Moderate depths 3-6 km	Compression to transpression with extensional (Shear Zones)	Steeply dipping	Ridely 2013; Maepa and Smith 2020	
	2-Turbidite-hosted	Bedding-parallel laminated quartz-carbonate veins in both folded and brittle-ductile shear zones, alongside extensive disseminated sulfides in sedimentary rock		Veins containing high-grade gold are located at the intersections with carbonaceous slates				Structurally and lithologically controlled	Cox et al., 1995; Ridely 2013; Boucher et al. 2015
	3-BIF-hosted	Discordant quartz veins and discordant banded disseminated to massive sulfide lenses		High average grade of about 5 g/t Au				Structurally controlled	Lawley et al. 2015; Morales et al., 2016; Adomako-Ansah et al., 2017
B-RIRGS	4-Reduced IR	Sheeted veins, massive, banded, disseminated and brecciated structures	Large (1MT to 10GT)	Variable ore grades ranging from 2.5 to 25 g/t Au	Structurally controlled	5 to 7 km	Compression with extensional (strike-slip faulting in fold and thrust belts)	Moderately to steeply dipping	Thompson and Newberry 2000; Hart 2007; Ridely 2013; Jia et al., 2019
C-OIRGS	5-HS Epithermal	Veins, hydrothermal breccia bodies, stockwork, and disseminations or replacements through irregular, inverted tear-drop, and veins upwards into wider 'mushroom heads' ore bodies.	Variable size 10,000T to > 1 GT, but usually small	Exceptional high grades up to 400 g/t, while the mean grade is around 3 g/t	Structurally controlled	Shallow depth (<2 km)	Dominantly extensional may be followed by compression	Commonly steeply dipping	Sillitoe 1993; Arribas 1995; Ruggieri et al., 1997; Ridely 2013
	6-Cu-Au porphyry	Semicircular to elliptical igneous bodies with stockwork-disseminated sulfides and mineralized quartz veinlets.	Giant (minimum 1 Mt up to 10 GT)	Low grade around 1 g/t Au	Structurally controlled (related to regional structures); Mineralization is predominantly found in the upper portion of small stocks	Shallow depths (1-4 km)	Compressional arc segments	No definite ore body	Heinrich et al. 2005; Rohrlach and Loucks 2005; Ridely 2013
	7-Au skarn	Disseminated to massive sulfide irregular lenses, veins to tabular or stratiform cutting skarn	Small, few larger deposits (25 to 2000 MT)	> 1 to 8 g/t Au	Combinations of lithological and structural features	Variable but commonly shallow	Transition from compressional to extensional regimes in the geodynamic history of a collisional orogenic system	Variable, most commonly stratiform	DeWitt et al., 1986; Theodore, 1990; Ridely 2013; Chen et al., 2007





D- Other types	8-LS Epithermal	Quartz-dominated with adularia and calcite veins with disseminated-stockwork sulfides; also occur as breccia pipes.	Typically, the veins are small, with large veins reaching a maximum thickness of 10 m.	Highly variable within the same ore body from 0.5 to 30 g/t Au	Structurally controlled	Shallow more than 1 Km depth	Extensional arc setting	Steeply dipping	Ridely 2013; Prihatmoko and Idrus, 2020
	9-Carlin-type	Disseminated sulfide minerals within discordant breccia as well as in stratiform and strata-bound deposits	Usually small around 7 Mt	Usually high grade ranging from 0.5 – 30 g/t	Structurally controlled (localized by high-angle faults)	Shallow to moderate depth (1-6 KM)	Correspond to a transition from compression to extension	Steeply dipping faults	Bagby and Berger, 1985; Muntean et al 2011; Ridely 2013; Hofstra and Cline, 2000
	10-Au-VMS	Banded and stratiform massive to semi-massive, rarely disseminated sulfide podiform to lenticular and adjacent stockwork zones	Small to moderate (1-50 MT); rarely giant deposits up to 150 MT	Usually low (0.5-1 g/t) but auriferous deposits contain >4 g/t Au	Structurally controlled and along contacts of rock units	Shallow depth of less than about 1500 m in the oceans	Extensional rifting setting	Horizontal sulfide lens while the lower stinger zone is nearly vertical	Hannington et al., 1999; Franklin et al., 2005; Galley et al., 2007; Ridely 2013; Piercey et al., 2023
	11-Polymetallic vein-type	Veins with disseminated-stockwork- breccia sulfides	The range of sizes varies from small, nearly 10,000 T, to very large, reaching 30 to 40 MT	0.5 -10 g/t Au; average 5 g/t	Litologically and structurally controlled in zones of high permeability, intrusive contacts, fault junctions, and breccia bodies and concentrated in zones of local domal uplift.	Shallow, few kilometers depth in the crust	Extensional tectonic regime	Steeply dipping	Cox and Singer, 1986; Morris and Cox, 1986; Ridely 2013; Maffini et al., 2017
	12-IOCG	Pipe- to funnel-like body with extensive hematite-rich breccia-vein sheets within the host stratigraphy	Small; rare large deposits (> 2 Gt)	<u>Magmatic IOCG</u> often compact in size and higher grade 1.5 g/t Au; <u>Hybrid IOCG</u> generally low grade 0.5 g/t; <u>Non-magmatic IOCG</u> high to low grade	Replacement ore bodies is likely to occur at the intersections of structural features and carbonate rock layers.	Variable depth of emplacement of the source batholith	Extensional or neutral tectonic regimes related to arc structures, few examples formed in compressional settings or rifting	Steeply dipping	Corriveau 2007; Hunt et al., 2007; Barton 2009; Storey, and Smith 2017; Skirrow 2022





Table 3. Mineralogical characteristics of the studied gold deposits.

Ore type	Ore Mineralogy	Metal association	Alteration mineralogy	Gangue mineralogy	Ore texture	Selected references	
A-Orogenic	1- Greenstone-hosted	Pyrite, pyrrhotite or arsenopyrite, chalcopyrite, sphalerite, free gold	Au, Ag, Cu, Zn, Pb, Bi, Hg, Sb, Te, W ± As, Mo; Au:Ag = 5:1 to 10:1	Carbonatization and sericitization	Quartz, carbonates, sericite, chlorite, amphibole, biotite, tourmaline	Disseminated - stockwork	Knopf 1929; Robert et al 1997; Pal and Mishra 2002; Wyman et al., 2016; Maepa and Smith 2020
	2- Turbidite-hosted	Pyrite, arsenopyrite, galena, gold	Au, Ag, Fe, As, Pb, Zn, ±Cu, ±Sb, ±Bi-Te-W	Sericitization and silicification	Quartz, ankerite, sericite, chlorite, carbonaceous matter, with minor plagioclase	Laminated-banded	Boyle 1986; Cox et al. 1991; Robert et al 1997; Haerberlin et al 2004
	3- BIF-hosted	Hematite and magnetite, little or no goethite; martite-goethite, pyrite, pyrrhotite, rare sphalerite, free gold, gold tellurides	Au, Ag, Pb, Zn, As, ±Cu	Sulfidation and chlorite – Carbonate alteration	Quartz, sericite, carbonaceous matter	Disseminated, brecciated	Caddey et al., 1991; Robert et al., 1997; Adomako-Ansah et al., 2017
B- Reduced intrusion-related	4- RIRG	High-temperature sulfide assemblages primarily consist of pyrrhotite and chalcopyrite, whereas lower-temperature assemblages are characterized by a predominance of arsenopyrite along with a variety of minerals and alloys containing bismuth, tellurium, antimony, lead, and gold.	Au-Bi-Te-As (W, Mo, Sb)	K-silicate alteration argillic alteration	K-feldspar, sericite, carbonates, overprinting plagioclase and mafic minerals	Disseminated/ stockwork	Bamford, 1972; Robert et al., 1997; Diment and Craig, 1998; Lindsey, 2000; Thompson and Newberry 2000; Maloof et al., 2001; Jia et al 2019
C- Oxidized intrusion-related	5-HS epithermal	Pyrite, enargite (or its low-temperature dimorph luzonite), tetrahedrite, tennantite, covellite, native gold or electrum, marcasite, chalcopyrite, sphalerite, and galena. Famatinite in some deposits. Sparse bomite, cassiterite, molybdenite, cinnabar, orpiment, realgar, stibnite, and wolframite. Minor amounts of Pb-, Ag-Pb, Bi- and Sn-bearing sulfosalts.	<u>Shallow:</u> Au, Ag, As, Sb, Se, Hg, Tl, low Ag:Au ratio, <0.1-1 % base metals <u>Deep:</u> Ag, Au, Pb, Zn, Ba, Mn, Se, Ag:Au=2:10 (> 20% base metals)	Silicification and grading into argillic, advanced argillic, or propylitic	Barite, anhydrite and alunite, K-feldspar, albite, sericite, chlorite, carbonate, quartz, amphibole, pyroxene, biotite and apatite, olivine, fluorite, ilvaite, garnet, monazite, perovskite, phlogopite, rutile, sphene, scapolite, and tourmaline.	Disseminated-stockwork + euhedrally terminated cavity-filling textures in veins	Heald et al., 1987; Arribas 1995; White and Hedenquist 1995; Robert et al 1997; Corriveau, 2007
	6- Cu-Au porphyry	Pyrite, chalcopyrite, bornite, rarely chalcocite, native or refractory gold. Molybdenite is the singular molybdenum ore mineral	Cu, W, Mo and Pb-Zn	The core exhibits sericitization and chloritization, which is subsequently succeeded by potassic, phyllic, advanced argillic, and	Quartz, K-feldspar, biotite, muscovite or sericite, chlorite, magnetite, epidote, anhydrite, and calcite	Disseminated-stockwork	Fyles, 1984; Robert et al., 1997; Zheng et al., 2020





				propylitic alterations.			
	7-Au-skarn	Pyrite, chalcopyrite, pyrrhotite, arsenopyrite, magnetite, hematite, sphalerite, galena, bismuthinite or native Bi-Te minerals, molybdenite, scheelite, native gold or electrum	Au, Ag, Cu, As, Pb, and Zn; as well as Bi, Co, Sb, Te, Se, and Cd	Retrograde alteration , some deposits show propylitic and phyllic alteration	Carbonates, diopside, garnet, wollastonite	Coarse-grained Massive-semi massive	Robert et al., 1997; Meinert, 1998
D- Other types	8- LS epithermal	Very variable mineralogy according to sulfidation state: <u>Intermediate-sulfidation-state</u> : Pyrite and marcasite are the primary sulfide ores; <u>low-sulfidation-state</u> : both pyrrhotite and arsenopyrite in ores with base-metal sulfides (galena, sphalerite and chalcopyrite), stibnite, rhodochrosite in some deposits, native Au or electrum, Ag hosted in electrum, acanthite and silver sulfosalts like proustite and pyrargyrite.	<u>Shallow</u> : Au, Ag, Cu leached (Hg overprint) <u>Intermediate</u> : Cu, Au, Ag, Bi, Te, Sn <u>Deep</u> : Cu, Au	Sericite-illite/Sericite-adularia; silicification; propylitic alteration	Quartz-dominated with adularia	Disseminated-stockwork	Heald et al. 1987; White and Hedenquist 1995; Ridely 2013
	9- Carlin-type	Pyrite, arsenian pyrite, arsenopyrite, marcasite, invisible gold, visible gold, stibnite, orpiment, realgar	As, Sb, Hg, Tl, Au:Ag ratio > 1, and very low base metal values	Decalcification and silicification	Quartz, calcite, serpentines	Disseminated-stockwork	Robert et al., 1997; Berger and Bagby 1991; Ridely 2013
	10- Au-VMS	Pyrite, arsenopyrite, sphalerite, chalcopyrite, galena, bornite, tennantite, tetrahedrite, mawsonite, Pb-Sb and Ag-Sb sulfosalts, native Bi, Bi tellurides, Ag and Au tellurides, electrum and occasional selenides	Cu, Se, Bi through Zn, Pb to Ag, Cu, As, Sb, Hg.	Sericitization, silicification, chloritization, epidotization, and aluminous acid alteration causing advanced argillic alteration	Quartz, barite	Massive to semi-massive and disseminated-stockwork	Poulsen and Hannington 1996; Robert et al., 1997; Dubé et al., 2007; Ridely, 2013
	11- Polymetallic vein-type	Pyrite, sphalerite, galena, argentite, electrum ±enargite ±digenite, chalcopyrite, pyrrhotite, tetrahedrite, barite, hessite, petzite, pyrargyrite ±bornite ±arsenopyrite	W, Bi, Sn, Mo, Cu, Pb, Zn, As, Ag, Zn, Cu, U, Au, Ag; with distinct metal zonation from the center of the pluton outwards with vein ore periphery.	Chlorite– sericite, silicification, and carbonate alteration	Fluorite, calcite and quartz	Colloform textures, disseminated, and small massive pods	Robert et al., 1997; Ridely, 2013
	12- IOCG	Magnetite, hematite-chalcopyrite-bornite-chalcocite and pyrrhotite	Ag, Au, Fe, Bi, Cu, U, Te ± As ± Co	Na alteration, Na-Ca alteration, Ca-Fe alteration, Fe-K alteration, and Poor Mg-rich alteration	Quartz ±biotite–actinolite–chlorite.	Brecciated, massive to pegmatoidal and spherulitic magnetite	Robert et al., 1997; Weihed et al., 2005; Ridely, 2013; Skirrow, 2022





Table 4. Ore-forming environment of the studied gold deposit types.

Ore type		Salinity	Fluid inclusion composition	Temperature	Pressure	Ore-forming depth	Sulfur isotopes	Oxygen isotopes	Selected References
A-Orogenic	1- Greenstone-hosted	Generally low salinity (<10 wt.% equiv. NaCl) but may show variable salinities (5 to 60 wt.% NaCl equiv.)	H ₂ O-CO ₂ -NaCl	T _h range from 180° to 360°C; gold deposition occur at temperatures near 350°C,	1 to 2 kbars.	~3 to 7 km	The δ ³⁴ S _{pyrite} usually have +Ve means, ranging from +1.8‰ to +4.7‰ (metamorphic ore fluid); rare negative values (-4 to -2‰).	δ ¹⁸ O _{quartz} = +11.6 to +14.7‰ δ ¹⁸ O _{water} = +4.4 to +9.8‰	Barrie and Touret 1999; Pal and Mishra 2002; Shelton et al., 2004; Zoheir and Weighed 2014
	2- Turbidite-hosted	Low salinity (0.1-10 wt.% NaCl equiv.)	H ₂ O-CO ₂ -NaCl type rich of CO ₂ (6 to 12 mole%)	T _h between 160 and 385 C; trapping temperatures near to 300 C	Trapping Pressure= 2.0±0.5 kbar	~ 2 to 10 km	δ ³⁴ S _{pyrite} commonly between -3 and +3‰ prefer the magmatic source of hydrothermal fluids	δ ¹⁸ O _{quartz} = +15.9 to +17.2 ‰	Nand 1989; Seccombe et al. 1993; Cox et al. 1995; Gao and Kwak 1995; Ramsay et al., 1998; Jia et al., 2001; Mernagh 2001
	3- BIF-hosted	Low salinity 2-10 NaCl equiv. (average ~3 wt.%)	H ₂ O-CO ₂ ±CH ₄ -NaCl	200 to 330 °C fluid inclusion trapping T 220 to 380°C (average 250°C)	0.5 to 2 kbar	5 to 7.5 km	Pyrites and pyrrhotites have δ ³⁴ S from - 15 to + 2.0‰	δ ¹⁸ O _{quartz} = +6.8 to +10.6 δ ¹⁸ O _{water} = +6.6 to +7.9‰ δ ¹⁸ O _{magnetite} = -1 to +8 ‰ Indicating evolved magmatic-hydrothermal fluid source	Andrianjakavah et al., 2007; Böhn et al 2012; Morales et al 2016; Adomako-Ansah et al., 2017; Ngiamte et al., 2023
B-Reduced intrusion-related	4- RIRG	Shallow environments: immiscible brine with concentrations > 30 wt. % NaCl equiv., alongside low-salinity CO ₂ -rich fluids with NaCl equivalent is < 5 wt. %. Certain deposits are subsequently influenced by brines with moderate to high salinity levels, ranging from 10 to 40 wt. % NaCl equiv. <u>Deeper environments:</u> low-salinity <10 wt. % NaCl equiv.	<u>Shallow environment:</u> immiscible brine vapor commonly contains CO ₂ ; <u>Deeper environments:</u> carbon dioxide-rich aqueous fluids	Range from 620° to 215°C. <u>Shallow environment:</u> high-temperature (>350°C); <u>Deeper environments:</u> (<350°C)	Range from <1 to 2 kbar Shallow < 1.3 kbar; deeper > 1.3 kbar	Shallow crustal settings (~<5 km) deeper crystallize at 5 to 7 km	Variable (mainly negative -11 to +2‰); <u>intrusion-hosted quartz Au-W-Bi-Te veins:</u> 0 to -3; <u>skarn mineralization:</u> 2 to -7; <u>country rock-hosted arsenopyrite veins:</u> -7 to -10; <u>Ag-Pb-Zn veins:</u> -9 to -11 per mil. signifies a continuous interaction with the sedimentary country rocks as the hydrothermal system matures and cools down over time.	<u>Au-W-Bi-Te sheeted quartz veins:</u> +14 to +16 ‰; <u>Sb and Ag-Pb-Zn veins:</u> +17 to +20 ‰; <u>host granitic rocks:</u> +11 to +13 ‰; <u>host sedimentary rocks:</u> +13 to +16 reflecting extensive wall-rock interaction.	Thompson and Newberry, 2000; Baker and Lang, 2001; Baker 2002; Marsh et al., 2003; Mair et al., 2006; Hart 2007; Nutt and Hofstra 2007
C- Oxidized intrusion-related	5- HS epithermal	Low-salinity FIs ranging from 0.5 to 5.5 wt.% NaCl equiv. with occurrence of some magmatic high-salinity FIs ranging from 30 to 45 wt. % NaCl equiv.	> 99 mol.% H ₂ O, ~ 0.5 mol.% CO ₂ , few N ₂ and CH ₄	T _h 190–280°C	< 0.5 kbar	1-1.5 km	Exhibit a broad spectrum, ranging from -4 to +5‰, predominantly cluster between -3 and 0‰, suggests that the sulfur present in the hydrothermal fluids originated from magmatic volatiles.	δ ¹⁸ O _{quartz} values variety from +17‰ to +22 ‰	Long et al., 2005; Ruggieri et al., 1997; Ridely 2013; Wang et al., 2016; Zhong et al., 2018; Chen et al., 2020
	6- Cu-Au porphyry	The ascent of complex fluids with moderate salinity leads to the formation of two distinct fluids within the central parts of the pluton. The first type is a high-density brine, high salinity fluids with salt concentrations > 40 wt. %. The second type is a lower-density, lower-salinity aqueous-saline gas phase. The max salt concentration: 50 - 60 wt. %	Na, K, Fe, Cu, Pb, Zn and Mn chloride salts, few CO ₂ , and considerable concentrations of gases that contain sulfur, including SO ₂ and H ₂ S	<u>Max (magmatic):</u> ~ 750°C <u>Intermediate:</u> ~ 450°C <u>Min (veins):</u> ~ 320 °C	Max (magmatic): P >1 kbar Min (veins): 0.1 kbar	Min: ~2 km Form at shallow depths between 1 to 10 km	δ ³⁴ S of sulfide minerals is generally documented to be close to zero, ranging from -5.4 to +5.3‰, indicating a magmatic origin.	δ ¹⁸ O for Sodic-potassic alteration minerals: +6.0 to +10.5‰; <u>potassic alteration assemblages:</u> -1.7 to +2.3‰; <u>Sericite:</u> +2.1 to +4.1‰; <u>illite alteration:</u> -8.9 to -0.6‰; <u>advanced argillic alteration:</u> +4.6 to +6.5‰; <u>advanced argillic alteration with meteoric component:</u> -9.1 to -4.8‰ δ ¹⁸ O for quartz in quartz veins +1.5 to +9.43 ‰	Ohmoto 1986; Taylor 1987; Ulrich et al., 2001; Ridely 2013; Gregory 2017; Schirra et al., 2022; Fazel et al., 2023





		NaCl equiv., The intermediate concentration around 40 wt. % NaCl equiv., The min concentration is roughly 5 wt. % NaCl equiv.							
	7- Au-skarn	A) high-salinity up to 65 wt.% NaCl equiv. B) moderate- to low-salinity ranging from 23 to 2 wt. % NaCl equiv.	Aqueous fluids within garnet and epidote	A) high-temperature between 500°C to more than 600°C B) Lower-temperature between 510 to 300°C; Gold precipitation occur at moderate T of 380–470 °C, moderate- to low-salinity fluids between 1.6 to 16.5 wt. % NaCl equiv. trapped in garnet and quartz.	1–3 kbar	A) shallow depth 4-km B) Very shallow depth < 1 km	The sulfides associated with the propylitic assemblage exhibit a notable enrichment in $\delta^{34}\text{S}$, with an average value of +1.4 ‰. Conversely, the sulfides found within the phyllic assemblage demonstrate a relative enrichment in $\delta^{32}\text{S}$, yielding an average $\delta^{34}\text{S}$ of -1.3 ‰.	A) Skarn-type deposits: early skarn phase: $\delta^{18}\text{O}_{\text{H}_2\text{O}} = +8$ ‰ to +12 ‰ (average +9.5 ‰); magnetite phase: $\delta^{18}\text{O}_{\text{H}_2\text{O}} = +8$ ‰ to +13 ‰ (average +10.4 ‰); late skarn phase: $\delta^{18}\text{O}_{\text{H}_2\text{O}} = +7.5$ ‰ to +10 ‰ (average +8.5 ‰); quartz-sulfide phase: $\delta^{18}\text{O}_{\text{H}_2\text{O}} = +4$ ‰. Quartz-carbonate phase: $\delta^{18}\text{O}_{\text{H}_2\text{O}} = +3$ ‰ to +3.7 ‰. B) Vein-type hydrothermal deposits: early quartz-sulfide phase: $\delta^{18}\text{O}_{\text{H}_2\text{O}} = +6.8$ ‰; late quartz-sulfide phase: $\delta^{18}\text{O}_{\text{H}_2\text{O}} = +5.7$ ‰ to +2.4 ‰. $\delta^{18}\text{O}_{\text{quartz}}$ values between +6.2 ‰ and +11.5 ‰ for retrograde stage suggesting magmatic fluids.	Vallance et al., 2009; Ridely 2013; Soloviev et al., 2013, 2019; He et al., 2015; Wu and Kainan 2016; Shi et al., 2020
D- Other types	8-Au-VMS	Salinities close to seawater between 1.4 to 9.6 wt.% NaCl equiv.	<u>Gases:</u> CO ₂ , CH ₄ , N ₂ , H ₂ S, SO ₂ <u>Major cations:</u> Na, K, Mg, Ca; <u>Ore elements:</u> Fe, Cu, Zn, Pb, <u>Gangue elements:</u> Ba, Li, B, Sr, Rb, and <u>Major anions:</u> S, Cl, Br	Hydrothermal fluids discharge at temperatures in the range of 200–400 °C devoid of boiling. T _h quartz ~ 200 °C.	Low confining pressures 0.5 kbar	Approximately 5000 m water depth or more	Sulfides exhibit a wide spectrum of $\delta^{34}\text{S}$ values, ranging from -6.5 to +15 ‰. The sulfides associated with early, lower temperature Zn-Pb-sulfosalts display the lowest mean $\delta^{34}\text{S}$ values at +4.6 ‰, while the highest $\delta^{34}\text{S}$ values are found in the late-stage, high-temperature, copper-rich sulfide assemblages.	$\delta^{18}\text{O}_{\text{quartz}} = 13.7$ to 16.4 ‰ for quartz from stringer and stockwork ores; and $\delta^{18}\text{O}_{\text{quartz}} = 8.0$ to 17 for quartz from felsic volcanics	Zengqian et al., 2001; Boulanger et al., 2010; Shanks and Thurston 2012; Gill et al., 2019; Tajeddin et al., 2019
	9- LS epithermal	< 1 to 10 wt.% NaCl equiv.	Aqueous-carbonic may be liquid-rich and /or vapor-rich inclusions	< 220-280 °C	Very low pressure <0.001 kbar	<1 km (500-800 m)	The $\delta^{34}\text{S}_{\text{pyrite}}$ range between -3 and +4.2 ‰. Propylitic alteration assemblage shows higher $\delta^{34}\text{S}$, with values (+3.1 and +4.2 ‰), than argillic alteration (-0.1 to +1.6 ‰) (mixed meteoric, mantle or evolved crustal, and magmatic fluids)	$\delta^{18}\text{O}_{\text{quartz}} = +2$ to +8 ‰; $\delta^{18}\text{O}_{\text{H}_2\text{O}} = -10.7$ to -5.7 ‰, with most of the samples express $\delta^{18}\text{O}_{\text{water}}$ values between -8 and -10 ‰ are comparable to the meteoric water value	Scott and Watanabe 1998; Sanger-von Oepen et al., 1990; Sholeh et al., 2016; An and Zhu 2018
	10- Carlin-type	About 0 to 7 wt.% NaCl equiv. low salinity (mostly around 6 wt.% NaCl equiv.)	Aqueous fluids express low but detectable CO ₂ (<4 mol. %) and H ₂ S	~ 150 to 250 °C	2.3 – 4 kbar	Formation depth <3 km	$\delta^{34}\text{S}_{\text{pyrite}}$ shows wide range from about 0 ‰ to > +10 ‰ (-3.8 to +11.5) due to contamination from sedimentary S.	For the ore body: $\delta^{18}\text{O}_{\text{calcite}}$ values (20.6–22.4 ‰); the country rocks express $\delta^{18}\text{O}$ values between 18.8 to 21.4 ‰ $\delta^{18}\text{O}_{\text{quartz}} +3.2$ to +27.8	Muntean et al., 2011; Bodnar et al., 2014; Tan et al., 2017; Yan et al., 2020; Lin et al., 2021
	11- Polymetallic vein-type	low to moderate (<13 equiv. wt.% NaCl) for all stages	Inclusions rich in CO ₂ in the early veins with few Fe, Cu, Pb, Zn, and S	Wide range of temperatures; <u>W deposits:</u> 500–600 °C, <u>Pb–Zn–Cu deposits:</u> about 250 °C	Very low; few bars up to 600 bar	From 4.5 km to several hundred meters below paleosurface	$\delta^{34}\text{S}_{\text{sulfides}}$ +0.8 ‰ to +3.6 ‰; point to a probable magmatic origin for the sulfur	$\delta^{18}\text{O}_{\text{quartz}}$ range between +12.5 and +14.8 ‰.	Rice et al., 1985; Dejonghe et al., 2002; Catchpole et al., 2011; Jovic et al., 2011; Mehrabi et al., 2019
	12- IOCG	<u>Magmatic IOCG:</u> high-salinity (30 – 55 NaCl equivalent); <u>Non-magmatic IOCG:</u> low to moderate salinities (3-42 NaCl equiv.); <u>Hybride IOCG:</u> moderate salinity (18-42 NaCl equiv.)	H ₂ O-NaCl-CaCl ₂ -CO ₂ ± MgCl ₂ ± FeCl ₂ system Aqueous-carbonic fluids carbonic ± CH ₄ rich in Na, Cl, Ca, K, Fe, and Ba, as well as elevated concentrations of Mn, Sr, Cu, Zn, and Pb.	Highly variable, but usually high T (up to 600 °C for oxide stage) changing to moderate T (500 – 300 °C for sulfide stage); <u>Magmatic IOCG:</u> moderate to high T (450° and 550 °C)	1.5-3.5 kbar.	About 7.5 to 9.0 km	$\delta^{34}\text{S}$ sulfides of all stages range between -3.5 to 2.6 ‰ comparable to the magmatic sulfur range. The weak negative $\delta^{34}\text{S}$ values between - 3.5 ‰ to - 1.5 ‰, perhaps indicate the addition of organic sulfur.	$\delta^{18}\text{O}_{\text{magnetite}}$ values of +1 to +8 ‰	Pollard, 2000; Hunt, 2005; Niiranan, 2005; Hunt et al., 2007; Rodriguez-Mustafa et al., 2020; Liang et al., 2021



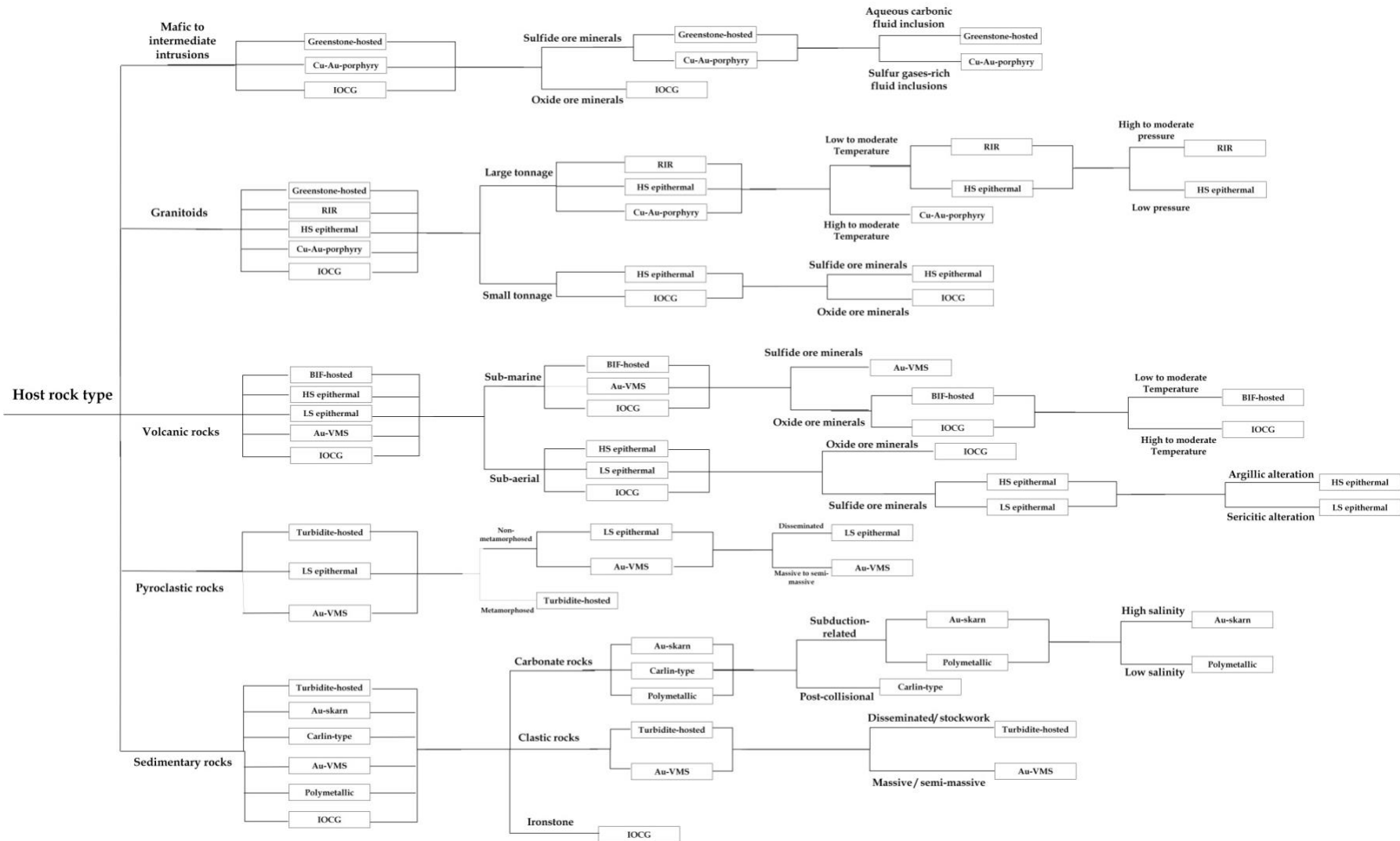


Figure. 5. Decision tree algorithm pattern that considers mixed parameters, which enables the differentiation between the various deposit types under study.

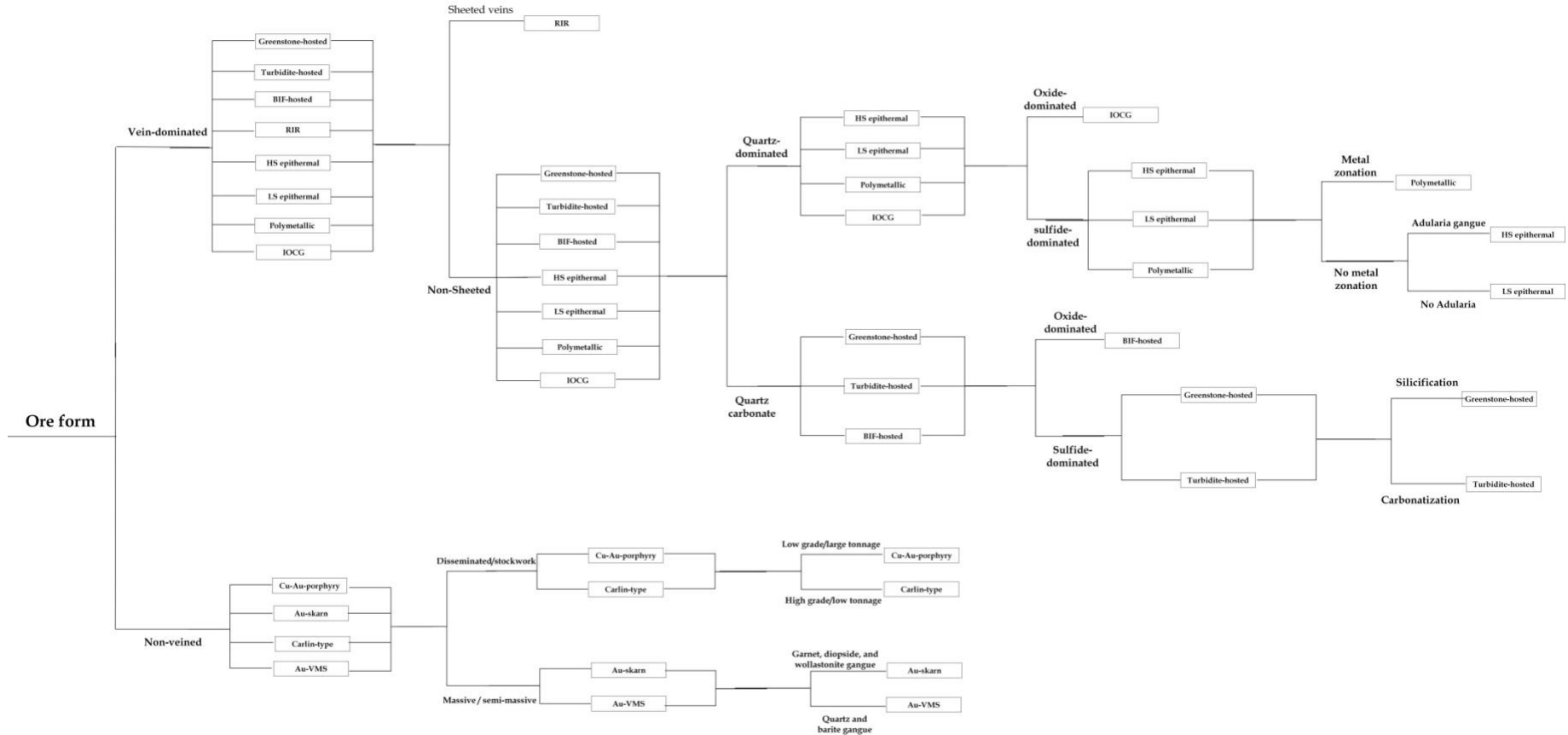


Figure. 6. Decision tree algorithm pattern based on ore body characteristics for distinguishing between the studied gold deposits.



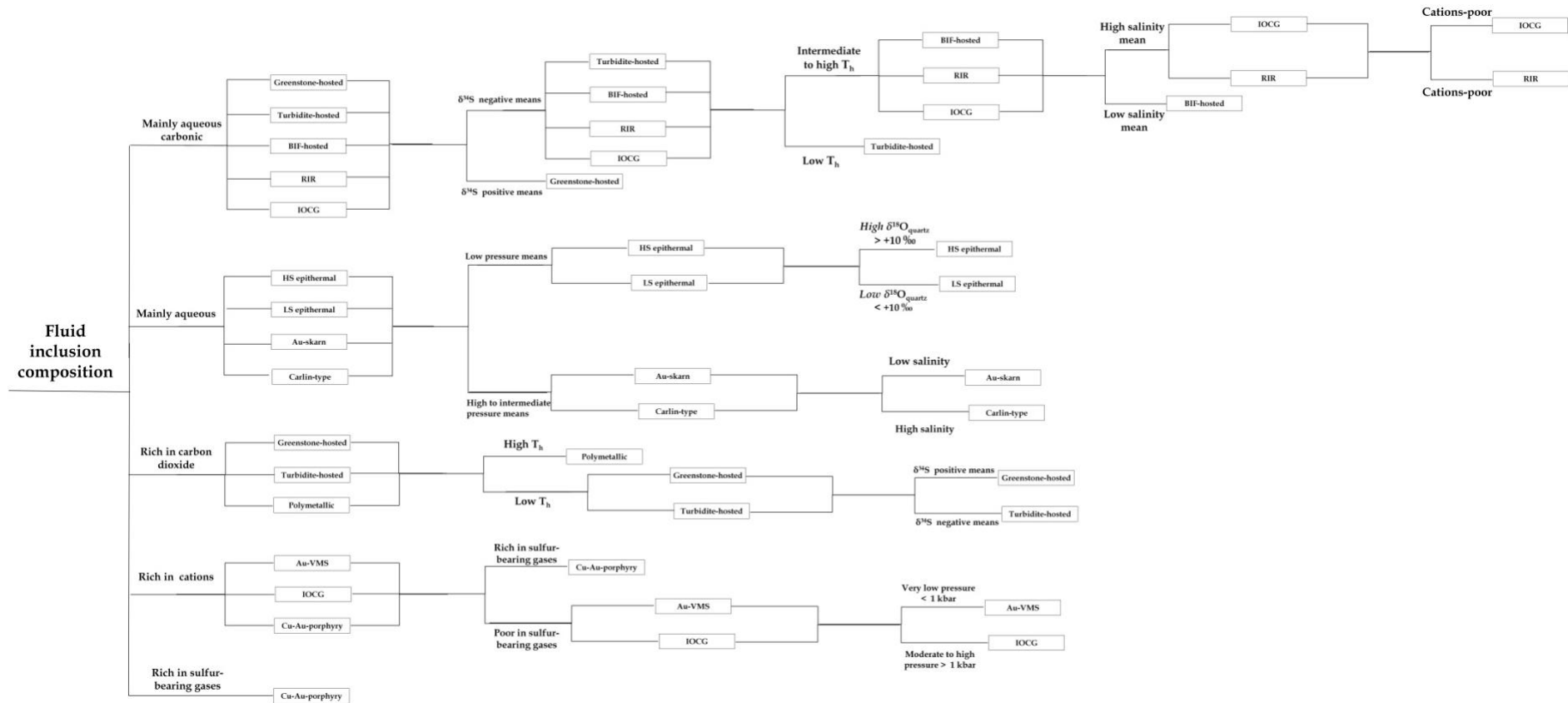


Figure. 7. Decision tree algorithm pattern based on the parameters of the ore-forming environments for distinguishing between the studied gold deposits.



7.5. Final Decision

After user finish with all the decision trees, the program will check for consistent classifications across the trees and provide a final classification for the gold deposit type if there is consistency and you can go through the validation test for the output to check and be sure what gold you have. Here is a sample interaction with the program for decision tree 1 (Figure. 9).

```
(a) System.out.println("choose what tree you want to decide based on");
System.out.println("1. Decision tree 1 - based on mixed parameters ");
System.out.println("2. Ore body characteristics decision tree ");
System.out.println("3. Based on ore-forming environment parameters ");
int Tree = scanner.nextInt();

(b) if(Tree == 1){
    System.out.println("What is the type of the host rock?");
    System.out.println("1. Mafic to intermediate intrusions");
    System.out.println("2. Granitoids");
    System.out.println("3. Volcanic rocks");
    System.out.println("4. Pyroclastic rocks");
    System.out.println("5. Sedimentary rocks");
    int hostRockType = scanner.nextInt();

    switch (hostRockType) {
        case 1:
            handleMafic(scanner);
            break;
        case 2:
            handleGranitoids(scanner);
            break;
        // Additional cases omitted for brevity
        default:
            System.out.println("Please choose only from the list");
    }
}

(c) else if(Tree == 2){
    System.out.println("What is the main nature of ore body?");
    System.out.println("1. Vein-dominated");
    System.out.println("2. Non-veined");
    int ore_form = scanner.nextInt();
    switch(ore_form){
        case 1:
            handleVein_dominated(scanner);
            break;
        case 2:
            handleNonVein_dominated(scanner);
            break;
        default:
            System.out.println("Please choose only from the list");
    }
}

(d) else if(Tree == 3){
    System.out.println("What is the main composition of the fluid incl");
    System.out.println("1. Mainly aqueous carbonic");
    System.out.println("2. Mainly aqueous");
    System.out.println("3. Rich in carbon dioxide");
    int compose = scanner.nextInt();
    switch(compose){
        case 1:
            handleMainlyAqueousCarbonic(scanner);
            break;
        case 2:
            handleMainlyAqueous(scanner);
            break;
        // Additional cases omitted for brevity
        default:
            System.out.println("Please choose only from the list");
    }
}
```

Figure. 8. Constructed code on Java for: (a) selecting the preferred decision tree; (b) the first step of decision tree 1 to choose the type of host rock; (c) the first step of decision tree 2 to choose the nature of the ore body; (d) the first step of decision tree 3 to choose the composition of the fluid inclusion.

```
choose what tree you want to decide based on
1. Decision tree 1 - based on mixed parameters
2. Ore body characteristics decision tree
3. Based on ore-forming environment parameters
> 1

What is the type of the host rock?
1. Mafic to intermediate intrusions
2. Granitoids
3. Volcanic rocks
4. Pyroclastic rocks
5. Sedimentary rocks
> 2

How is the tonnage of the ore body?
1. Large tonnage
2. Small tonnage
> 1

How is the ore-forming temperature?
1. Low to moderate Temperature
2. High to moderate Temperature
> 1

How is the ore-forming pressure?
1. High to moderate pressure
2. Low pressure
> 2

HS epithermal
Try again?
1. YES
2. NO, get back to other decision tree
> 2
```



Figure. 9. Sample of interaction with the program using decision tree 1 to identify a HS epithermal deposit.

7.6. Confirmation the results

In the case that two or three decision trees yield identical outcomes, users have the option to validate the result by responding to inquiries pertaining to the specific type of gold deposit that was identified.

CONCLUSION

Many gold deposits are recognized in the literature; most of them share many similar characteristics, although they have different tonnages and grades. For example, RIRGs share a lot of similar characteristics with orogenic gold deposits, including high contents of W, Bi, and Te; reduced sulfide association; low salinity; CO₂-bearing fluids; lodes formed subsequent to the maximum metamorphic conditions; and sequential/spatial relations with granitic rocks (Sillitoe and Thompson 1998). Distinguishing among them became a serious problem for many researchers and mining companies and represents a vital role in the formulation of exploration plans, the assessment of potential sites, and the execution of resource evaluations for chosen prospects. The instrumental advances and deep understanding of each gold mineralization type resulted in broadening the terms of the previously recognized types, the introduction of new gold deposits, and overlapping with other types. The resemblances found among various gold deposits are linked to their role as different facets of larger hydrothermal systems that are active at equivalent crustal levels and are genetically interconnected. This work presents the comprehensive features of a diverse groups of gold deposits, which vary in terms of their geological, mineralogical, and geochemical characteristics as well as their formation conditions. We selected 12 of the most common and similar gold mineralization types, either major or minor, to distinguish among them on the basis of their main geological field attributes and mineralogical in addition to the ore-forming environment parameters. We utilized the classification scheme of Robert et al. (2007) with minor differences. According to them, gold mineralizations can be grouped into four classes: (a) the orogenic gold class, which includes three types, namely greenstone-hosted gold, turbidite-hosted gold, and BIF-hosted; (b) the reduced intrusion-related gold class; (c) the oxidized intrusion-related gold class, which includes HS epithermal, Cu-Au porphyry, Au-skarn, and LS epithermal; (d) additional gold deposit types, including Carlin-type, Au-VMS, polymetallic vein-type gold deposits, and IOCG. This study proposes a computer-based approach that incorporates a great number of variable parameters for identifying the gold deposit type. The decision-making process involves three distinct decision trees, followed by validation questions to confirm the resulting gold deposit type. The implementation of decision trees using Java allowed a systematic and reproducible classification, aiding geologists in making informed decisions about gold deposit types. The interactive nature of the program ensures that all necessary geological features are considered, making the classification process thorough and detailed.

REFERENCE

- Abd El Monsef, M., and A. Abdelnasser (2021), Ore-forming mechanism and its relationship with deformational and metamorphic episodes at Haimur gold mine, Nubian Shield, Egypt, *Geological Magazine*, 158(3), 518-536.
- Adomako-Ansah, K., T. Mizuta, D. Ishiyama, and N. Q. Hammond (2017), Nature of ore-forming fluid and formation conditions of BIF-hosted gold mineralization in the Archean Amalia Greenstone Belt, South Africa: Constraints from fluid inclusion and stable isotope studies, *Ore Geology Reviews*, 89, 609-626.
- An, F., and Y. Zhu (2018), Geology and geochemistry of the Early Permian Axi low-sulfidation epithermal gold deposit in North Tianshan (NW China), *Ore Geology Reviews*, 100, 12-30.
- Andrianjakavah, P., S. Salvi, D. Béziat, D. Guillaume, M. Rakotondrazafy, and B. Moine (2007), Textural and fluid inclusion constraints on the origin of the banded-iron-formation-hosted gold deposits at Maevatanana, central Madagascar, *Mineralium Deposita*, 42, 385-398.
- Angeles, C. A., S. Prihatmoko, and J. S. Walker (2002), Geology and alteration-mineralization characteristics of the Cibaliung epithermal gold deposit, Banten, Indonesia, *Resource Geology*, 52(4), 329-339.
- Arribas Jr, A. (1995), Characteristics of high-sulfidation epithermal deposits, and their relation to magmatic fluid, *Mineralogical Association of Canada Short Course*, 23, 419-454.
- Bagby, W. C., and B. R. Berger (1985), Geologic characteristics of sediment-hosted, disseminated precious-metal deposits in the western United States.





- Baker, T. (2002), Emplacement depth and carbon dioxide-rich fluid inclusions in intrusion-related gold deposits, *Economic Geology*, 97(5), 1111-1117.
- Baker, T., and J. R. Lang (2001), Fluid inclusion characteristics of intrusion-related gold mineralization, Tombstone–Tungsten magmatic belt, Yukon Territory, Canada, *Mineralium Deposita*, 36, 563-582.
- Bamford, R. W. (1972), The Mount Fubilan (Ok Tedi) porphyry copper deposit, Territory of Papua and New Guinea, *Economic Geology*, 67(8), 1019-1033.
- Barley, M., and D. Groves (1992), Supercontinent cycles and the distribution of metal deposits through time, *Geology*, 20(4), 291-294.
- Barrie, I. J., and J. L. Touret (1999), Fluid inclusion studies of gold-bearing quartz veins from the Yirisen deposit, Sula Mountains greenstone belt, Masumbiri, Sierra Leone, *Ore Geology Reviews*, 14(3-4), 203-225.
- Barrie, C., M. Hannington, and W. Bleeker (1997), The giant Kidd Creek volcanic-associated massive sulfide deposit, Abitibi Subprovince, Canada.
- Barton, M. (2014), Iron oxide (–Cu–Au–REE–P–Ag–U–Co) systems, *Treatise on geochemistry*, 515-541.
- Barton, M. D. (2009), IOCG deposits: A Cordilleran perspective, paper presented at Proc. 11th Biennial SGA Meeting, Citeseer.
- Barton, M. D., and D. A. Johnson (1996), Evaporitic-source model for igneous-related Fe oxide–(REE–Cu–Au–U) mineralization, *Geology*, 24(3), 259-262.
- Barton, M. D., D. A. Johnson, D. C. Kreiner, and E. P. Jensen (2013), Vertical zoning and continuity in Fe oxide (–Cu–Au–Ag–Co–UP–REE)(or ‘IOCG’) systems: Cordilleran insights, paper presented at Proceedings of the 12th Biennial Meeting, Society for Geology Applied to Ore Deposits.
- Berge, J. (2011), Paleoproterozoic, turbidite-hosted, gold deposits of the Ashanti gold belt (Ghana, West Africa): Comparative analysis of turbidite-hosted gold deposits and an updated genetic model, *Ore Geology Reviews*, 39(1-2), 91-100.
- Berger, B., and W. Bagby (1991), The geology and origin of Carlin-type gold deposits, in *Gold metallogeny and exploration*, edited, pp. 210-248.
- Berger, B. R., R. A. Ayuso, J. C. Wynn, and R. R. Seal II (2008), Preliminary model of porphyry copper deposits Rep. 2331-1258, US Geological Survey.
- Bodnar, R. (1995), Fluid-inclusion evidence for a magmatic source for metals in porphyry copper deposits, *Magma, fluid and ore deposit*, 139-152.
- Bodnar, R., and J. Cline (1991), Fluid inclusion petrology of porphyry copper deposits revisited: Re-interpretation of observed characteristics based on recent experimental and theoretical data, *Plinius*, 5, 24-25.
- Bodnar, R., P. Lecumberri-Sanchez, D. Moncada, and M. Steele-MacInnis (2014), 13.5–Fluid inclusions in hydrothermal ore deposits, *Treatise on geochemistry*, 13, 119-142.
- Boucher, R., A. Rossiter, R. Fraser, and D. Turnbull (2015), Review of the structural architecture of turbidite-hosted gold deposits, Victoria, Australia, *Applied Earth Science*, 124(3), 136-146.
- Boulanger, R., G. Chi, T. Skulski, and S. Castonguay (2010), Characterization and evolution of fluids associated with the Cu–Au deposit of the Ming Mine, Rambler area, northeast Newfoundland, Canada, edited, GeoCanada.
- Boyle, R. (1986), Gold deposits in turbidite sequence: their geology, geochemistry and history of the theories of their origin, *Turbidite-hosted Gold Deposits*, SJ, 1-13
- Bühn, B., R. V. Santos, M. A. Dardenne, and C. G. de Oliveira (2012), Mass-dependent and mass-independent sulfur isotope fractionation ($\delta^{34}\text{S}$ and $\delta^{33}\text{S}$) from Brazilian Archean and Proterozoic sulfide deposits by laser ablation multi-collector ICP-MS, *Chemical Geology*, 312, 163-176.
- Caddey, S. W., B. RL, T. Campbell, R. Reid, and R. Otto (1991), The Homestake gold mine, an early Proterozoic iron-formation-hosted gold deposit, Lawrence County, South Dakota, US Government Printing Office.
- Campbell, A. R., and P. B. Larson (1998), Introduction to stable isotope applications in hydrothermal systems.
- Castonguay, S., B. Dubé, P. Mercier-Langevin, V. McNicoll, W. Oswald, V. Janvier, and M. Malo (2015), Geological controls of BIF-hosted gold mineralization: Insights from the world-class Musselwhite (Ontario) and Meadowbank (Nunavut) deposits, Canada, paper presented at Mineral resources in a sustainable world, Proceeding book, 13 SGA Meeting, Nancy-France.





- Catchpole, H., K. Kouzmanov, L. Fontboté, M. Guillong, and C. A. Heinrich (2011), Fluid evolution in zoned Cordilleran polymetallic veins—insights from microthermometry and LA-ICP-MS of fluid inclusions, *Chemical Geology*, 281(3-4), 293-304.
- Chen, H. (2013), External sulphur in IOCG mineralization: Implications on definition and classification of the IOCG clan, *Ore Geology Reviews*, 51, 74-78.
- Chen, M. T., J. H. Wei, Y. J. Li, W. J. Shi, and N. Z. Liu (2020), Epithermal gold mineralization in Cretaceous volcanic belt, SE China: Insight from the Shangshangang deposit, *Ore Geology Reviews*, 118, 103355.
- Chen, Y.-J., H.-Y. Chen, K. Zaw, F. Pirajno, and Z.-J. Zhang (2007), Geodynamic settings and tectonic model of skarn gold deposits in China: an overview, *Ore Geology Reviews*, 31(1-4), 139-169.
- Corriveau, L., L. Ootes, H. Mumin, V. Jackson, V. Bennett, J. Cremer, B. Rivard, I. McMartin, G. Beaudoin, and B. Milkereit (2007), Alteration vectoring to IOCG (U) deposits in frontier volcano-plutonic terrains, Canada, paper presented at Proceedings of exploration, Citeseer.
- Cox, D. P. (1986), Descriptive model of polymetallic veins, *Mineral deposit models: US Geological Survey Bulletin*, 1693, 125.
- Cox, D. P., and D. A. Singer (1986), *Mineral deposit models Rep.*, USGPO.
- Cox, S., S. Sun, M. Etheridge, V. Wall, and T. Potter (1995), Structural and geochemical controls on the development of turbidite-hosted gold quartz vein deposits, Wattle Gully mine, central Victoria, Australia, *Economic Geology*, 90(6), 1722-1746.
- Cox, S., V. Wall, M. Etheridge, and T. Potter (1991), Deformational and metamorphic processes in the formation of mesothermal vein-hosted gold deposits—examples from the Lachlan Fold Belt in central Victoria, Australia, *Ore geology reviews*, 6(5), 391-423.
- de Haller, A., and L. s. Fontboté (2009), The Raúl-Condestable iron oxide copper-gold deposit, central coast of Peru: Ore and related hydrothermal alteration, sulfur isotopes, and thermodynamic constraints, *Economic Geology*, 104(3), 365-384.
- Dejonghe, L., B. Darras, G. Hughes, P. Muchez, J. S. Scoates, and D. Weis (2002), Isotopic and fluid-inclusion constraints on the formation of polymetallic vein deposits in the central Argentinian Patagonia, *Mineralium Deposita*, 37, 158-172.
- DeWitt, E., J. Redden, A. B. Wilson, D. Buscher, and J. Dersch (1986), Mineral resource potential and geology of the Black Hills National Forest, South Dakota and Wyoming with a section on salable commodities Rep., US Geological Survey.
- Diment, R., and S. Craig (1998), Brewery Creek gold deposit, central Yukon, *Yukon exploration and geology*, 1998, 225-230.
- Dubé, B., G. R. Dunning, and K. Lauziere (1998), Geology of the Hope Brook Mine, Newfoundland, Canada; a preserved late Proterozoic high-sulfidation epithermal gold deposit and its implications for exploration, *Economic Geology*, 93(4), 405-436.
- Dubé, B., P. Gosselin, P. Mercier-Langevin, M. Hannington, and A. Galley (2007), Gold-rich volcanogenic massive sulphide deposits, Geological Association of Canada, Mineral Deposits Division, 75-94.
- Dusel-Bacon, C., J. N. Aleinikoff, W. R. Premo, S. Paradis, and I. Lohr-Schmidt (2007), Tectonic setting and metallogenesis of volcanogenic massive sulfide deposits in the Bonfield Mining District, Northern Alaska Range, Recent US Geological Survey Studies in the Tintina Gold Province, Alaska, United States, and Yukon, Canada—Results of a, B1-B7.
- Einaudi, M., L. Meinert, and R. Newberry (1981), Skarn deposits.
- Eisler, R. (2004), Gold concentrations in abiotic materials, plants, and animals: a synoptic review, *Environmental monitoring and assessment*, 90, 73-88.
- Ettlinger, A. D., and L. D. Meinert (1991), Copper-gold skarn mineralization at the Veselyi mine, Siniukhinskoe district, Siberia, USSR, *Economic Geology*, 86(1), 185-194.
- Fazel, E.T., Mehrabi, B., Zamanian, H. and Hayatolghaybi, M., (2023). Fluid inclusions and C–H–O–S–Pb isotope systematics of the Senj Mo–Cu deposit, Alborz magmatic belt, northern Iran: implications for fluid evolution and regional mineralization. *Geological Magazine*, 160(1), pp.1-21.
- Fontboté, L., J. Vallance, A. Markowski, and M. Chiaradia (2005), Oxidized gold skarns in the Nambija District, Ecuador.
- Forster, D. B., P. K. Secombe, and D. Phillips (2004), Controls on skarn mineralization and alteration at the Cadia deposits, New South Wales, Australia, *Economic Geology*, 99(4), 761-788.





- Franklin, J., and R. Thorpe (1982), Comparative metallogeny of the Superior, Slave and Churchill provinces, Precambrian sulphide deposits HS Robinson Memorial Vol, Geol Ass Can Spec Pap, 3-90.
- Franklin, J., H. Gibson, I. Jonasson, and A. Galley (2005), Volcanogenic massive sulfide deposits: in Hedenquist, J.W., Thompson, J.F.H., Goldfarb, R.J., and Richards, J.P., eds., Economic Geology, 100th Anniversary Volume, The Economic Geology Publishing Company, 523-560.
- Fyles, J. T. (1984), Geological setting of the Rossland mining camp, Province of British Columbia, Ministry of Energy, Mines and Petroleum Resources.
- Galley, A. G., M. D. Hannington, and I. Jonasson (2007), Volcanogenic massive sulphide deposits, Mineral deposits of Canada: a synthesis of major deposit-types, district metallogeny, the evolution of geological provinces, and exploration methods, 5, 141-161.
- Gao, Z., and T. Kwak (1995), Turbidite-hosted gold deposits in the Bendigo-Ballararat and Melbourne Zones, Australia. I. Geology, Mineralization, stable isotopes, and implications for exploration, International Geology Review, 37(10), 910-944.
- Gill, S. B., S. J. Piercey, G. D. Layne, and G. Piercey (2019), Sulphur and lead isotope geochemistry of sulphide minerals from the Zn-Pb-Cu-Ag-Au Lemarchant volcanogenic massive sulphide (VMS) deposit, Newfoundland, Canada, Ore Geology Reviews, 104, 422-435.
- Goldfarb, R., L. Snee, L. Miller, and R. Newberry (1991), Rapid dewatering of the crust deduced from ages of mesothermal gold deposits, Nature, 354(6351), 296-298.
- Goldfarb, R. J., and I. Pitcairn (2023), Orogenic gold: is a genetic association with magmatism realistic?, Mineralium Deposita, 58(1), 5-35.
- Goldfarb, R. J., C. Hart, M. Miller, L. Miller, G. L. Farmer, and D. I. Groves (2000), The Tintina gold belt: a global perspective, British Columbia and Yukon Chamber of Mines, Special Volume, 2, 5-34.
- Gregory, M. J. (2017), A fluid inclusion and stable isotope study of the Pebble porphyry copper-gold-molybdenum deposit, Alaska, Ore Geology Reviews, 80, 1279-1303.
- Groves, D. I., F. P. Bierlein, L. D. Meinert, and M. W. Hitzman (2010), Iron oxide copper-gold (IOCG) deposits through Earth history: Implications for origin, lithospheric setting, and distinction from other epigenetic iron oxide deposits, Economic Geology, 105(3), 641-654.
- Groves, D. I., R. J. Goldfarb, M. Gebre-Mariam, S. Hagemann, and F. Robert (1998), Orogenic gold deposits: a proposed classification in the context of their crustal distribution and relationship to other gold deposit types, Ore geology reviews, 13(1-5), 7-27.
- Haeberlin, Y., R. Moritz, L. Fontboté, and M. Cosca (2004), Carboniferous orogenic gold deposits at Pataz, Eastern Andean Cordillera, Peru: geological and structural framework, paragenesis, alteration, and $40\text{Ar}/39\text{Ar}$ geochronology, Economic Geology, 99(1), 73-112.
- Hagemann, S. G., and P. E. Brown (2000), Gold in 2000, Society of Economic Geologists.
- Hammarstrom, J. M., B. B. Kotlyar, T. G. Theodore, J. E. Elliott, D. A. John, J. L. Doebrich, J. T. Nash, R. R. Carlson, G. K. Lee, and K. E. Livo (1995), Cu, Au, and Zn-Pb Skarn Deposits, Preliminary Compilation of Descriptive Geoenvironmental Mineral Deposit Models, US Geological Survey Open-File Report, 95-831.
- Hannington, M., and P. Herzig (1993), Shallow submarine hydrothermal systems in modern island arc settings, Geological Association of Canada; v, 19, p, A40.
- Hannington, M., K. Poulsen, J. Thompson, and R. Sillitoe (1997), Volcanogenic gold in the massive sulfide environment, in Barrie, C.T., and Hannington, M.D., eds., Volcanic-Associated Massive Sulfide Deposits: Processes and Examples in Modern and Ancient Settings: Reviews in Economic Geology 8, p. 325-356.
- Hannington, M. D., C. Barrie, and W. Bleeker (1999), The giant Kidd Creek volcanogenic massive sulfide deposit, western Abitibi subprovince, Canada: Summary and Synthesis.
- Harris, A. C., S. D. Golding, and N. C. White (2005), Bajo de la Alumbrera copper-gold deposit: Stable isotope evidence for a porphyry-related hydrothermal system dominated by magmatic aqueous fluids, Economic Geology, 100(5), 863-886.
- Hart, C., and R. Goldfarb (2005), Distinguishing intrusion-related from orogenic gold systems, paper presented at New Zealand Minerals Conference Proceedings.
- Hart, C. J. (2005), Classifying, distinguishing and exploring for intrusion-related gold systems, The Gangue, 87(1), 9.
- Hart, C. J. (2007), Reduced intrusion-related gold systems, Mineral Deposits of Canada: A synthesis of Major deposit types, district metallogeny, the Evolution of geological provinces, and exploration methods: Geological Association of Canada, Mineral Deposits Division, Special Publication, 5, 95-112.





- Hayward, N., R. G. Skirrow, and T. Porter (2010), Geodynamic setting and controls on iron oxide Cu-Au (\pm U) ore in the Gawler Craton, South Australia, Hydrothermal iron oxide copper-gold and related deposits: A global perspective, 3, 105-131.
- He, W.-Y., X.-X. Mo, Z.-H. He, N. C. White, J.-B. Chen, K.-H. Yang, R. Wang, X.-H. Yu, G.-C. Dong, and X.-F. Huang (2015), The geology and mineralogy of the Beiya skarn gold deposit in Yunnan, southwest China, Economic Geology, 110(6), 1625-1641.
- Heald, P., N. K. Foley, and D. O. Hayba (1987), Comparative anatomy of volcanic-hosted epithermal deposits; acid-sulfate and adularia-sericite types, Economic geology, 82(1), 1-26.
- Hedenquist, J. W., and R. Sillitoe (2003), Linkages between volcanotectonic settings, ore-fluid compositions, and epithermal precious metal deposits, Volcanic, geothermal, and ore-forming fluids, 315-343.
- Heinrich, C. A., W. Halter, M. R. Landtwing, and T. Pettke (2005), The formation of economic porphyry copper (-gold) deposits: constraints from microanalysis of fluid and melt inclusions, Geological Society, London, Special Publications, 248(1), 247-263.
- Hewitt, W., L. JF, R. Lorraway, K. Moule, R. PM, and S. HJ (1980), OK TEDI PROJECT-GEOLOGY OF PRINCIPAL ORE DEPOSITS.
- Hitzman, M. W., and T. Porter (2000), Iron oxide-Cu-Au deposits: What, where, when, and why, Hydrothermal iron oxide copper-gold and related deposits: A global perspective, 1, 9-25.
- Hitzman, M. W., N. Oreskes, and M. T. Einaudi (1992), Geological characteristics and tectonic setting of proterozoic iron oxide (Cu · U · Au · REE) deposits, Precambrian research, 58(1-4), 241-287.
- Hofstra, A. H., and J. S. Cline (2000), Characteristics and models for Carlin-type gold deposits.
- Hunt, J. (2005), The geology and genesis of iron oxide-copper-gold mineralisation associated with Wernecke Breccia, Yukon, Canada, James Cook University.
- Hunt, J., T. Baker, and D. Thorkelson (2007), A review of iron oxide copper-gold deposits, with focus on the Wernecke Breccias, Yukon, Canada, as an example of a non-magmatic end member and implications for IOCG genesis and classification, Exploration and Mining Geology, 16(3-4), 209-232.
- Huston, D. L. (2000), Gold in volcanic-hosted massive sulfide deposits: distribution, genesis, and exploration.
- Hutchison, W., A. A. Finch, and A. J. Boyce (2020), The sulfur isotope evolution of magmatic-hydrothermal fluids: Insights into ore-forming processes, Geochimica et Cosmochimica Acta, 288, 176-198.
- Ishihara, S. (1981), The granitoid series and mineralization.
- Jensen, E. P., and M. D. Barton (2000), Gold deposits related to alkaline magmatism.
- Jia, S., E. Wang, J. Fu, X. Wang, and W. Li (2019), Geology, fluid inclusions and isotope geochemistry of the Herenping gold deposit in the southern margin of the Yangtze Craton, China: a sediment-hosted reduced intrusion-related gold deposit?, Ore Geology Reviews, 107, 926-943.
- Jia, Y., X. Li, and R. Kerrich (2001), Stable isotope (O, H, S, C, and N) systematics of quartz vein systems in the turbidite-hosted Central and North Deborah gold deposits of the Bendigo gold field, central Victoria, Australia: Constraints on the origin of ore-forming fluids, Economic Geology, 96(4), 705-721.
- Jovic, S. M., D. M. Guido, I. B. Schalamuk, F. J. Ríos, C. C. Tassinari, and C. Recio (2011), Pingüino In-bearing polymetallic vein deposit, Deseado Massif, Patagonia, Argentina: characteristics of mineralization and ore-forming fluids, Mineralium Deposita, 46, 257-271.
- Keith, M., K. M. Haase, U. Schwarz-Schampera, R. Klemm, S. Petersen, and W. Bach (2014), Effects of temperature, sulfur, and oxygen fugacity on the composition of sphalerite from submarine hydrothermal vents, Geology, 42(8), 699-702.
- Kerrich, R. (1993), Perspectives on genetic models for lode gold deposits, Mineralium Deposita, 28, 362-365.
- Kesler, S. E. (2005), Ore-forming fluids, Elements, 1(1), 13-18.
- Khashgerel, B.-E., R. O. Rye, J. W. Hedenquist, and I. Kavalieris (2006), Geology and reconnaissance stable isotope study of the Oyu Tolgoi porphyry Cu-Au system, South Gobi, Mongolia, Economic Geology, 101(3), 503-522.
- Klemm, L. M., T. Pettke, C. A. Heinrich, and E. Campos (2007), Hydrothermal evolution of the El Teniente deposit, Chile: Porphyry Cu-Mo ore deposition from low-salinity magmatic fluids, Economic Geology, 102(6), 1021-1045.
- Knopf, A. (1929), The mother lode system of California, US Government Printing Office.





- Knutson, J., J. Ferguson, W. Roberts, T. Donnelly, and I. Lambert (1979), Petrogenesis of the copper-bearing breccia pipes, Redbank, Northern Territory, Australia, *Economic Geology*, 74(4), 814-826.
- Kuehn, C. A., and A. W. Rose (1995), Carlin gold deposits, Nevada; origin in a deep zone of mixing between normally pressured and overpressured fluids, *Economic Geology*, 90(1), 17-36.
- Kwan, K., I. Johnson, J. M. Legault, K. Khaled, and A. Prikhodko (2019), Understanding Archean greenstone-hosted lode gold mineralization in Ontario Canada through helicopter TDEM data, *ASEG Extended Abstracts*, 2019(1), 1-4.
- Lawley, C. J., B. Dubé, P. Mercier-Langevin, B. Kjarsgaard, R. Knight, and D. Vaillancourt (2015), Defining and mapping hydrothermal footprints at the BIF-hosted Meliadine gold district, Nunavut, Canada, *Journal of Geochemical Exploration*, 155, 33-55.
- Leube, A., W. Hirdes, R. Mauer, and G. O. Kesse (1990), The early Proterozoic Birimian Supergroup of Ghana and some aspects of its associated gold mineralization, *Precambrian research*, 46(1-2), 139-165.
- Li, J., K. QIN, and G. LI (2006), The basic characteristics of gold-rich porphyry copper deposits and their ore sources and evolving processes of high oxidation magma and ore-forming fluid, *Acta Petrologica Sinica*, 22, 678-688.
- Liang, P., L. Chen, R. Li, Y. Xie, C. Wu, and C.-K. Lai (2021), In-situ element geochemical and sulfur isotope signature of pyrite and chalcopyrite: Constraints on ore-forming processes of the Laoshankou iron oxide-copper (-gold) deposit, northern East Junggar, *Ore Geology Reviews*, 139, 104510.
- Lin, S., K. Hu, J. Cao, T. Bai, Y. Liu, and S. Han (2021), An in situ sulfur isotopic investigation of the origin of Carlin-type gold deposits in Youjiang Basin, southwest China, *Ore Geology Reviews*, 134, 104187.
- Lindsey, M. (2000), The magmatic and structural setting of the Brewery Creek gold mine, central Yukon, *Yukon Exploration and Geology* 1999.
- Long, X., N. Hayward, G. Begg, F. Minlu, W. Fangzheng, and F. Pirajno (2005), The Jinxi–Yelmand high-sulfidation epithermal gold deposit, Western Tianshan, Xinjiang Province, PR China, *Ore Geology Reviews*, 26(1-2), 17-37.
- Maepa, F. M., and R. S. Smith (2020), Examining the controls on gold deposit distribution in the Swayze greenstone belt, Ontario, Canada, using multi-scale methods of spatial data analysis, *Ore Geology Reviews*, 125, 103671.
- Maffini, M. N., K. Wemmer, S. Radice, S. Oriolo, F. D'Eramo, J. Coniglio, M. Demartis, and L. Pinotti (2017), Polymetallic (Pb-Zn-Cu-Ag±Au) vein-type deposits in brittle-ductile transtensional shear zones, Eastern Sierras Pampeanas (Argentina): Age constraints and significance for the Late Paleozoic tectonic evolution and metallogensis, *Ore Geology Reviews*, 89, 668-682.
- Mahmoud, A., V. Dyakonov, and A. Kotelnikov (2019), Genesis and evolution of the Hamama volcanic massive sulphide deposits, Egypt, paper presented at IOP Conference Series: Materials Science and Engineering, IOP Publishing.
- Mahmoud, A., V. Dyakonov, A. Kotelnikov, M. Dawoud, and H. El-Dokouny (2021), Vertical Zoning and Geochemical Anomaly Fields of the Hamama Gold Deposit in the Central Part of Egypt's Eastern Desert, *Geology of Ore Deposits*, 63(2), 156-171.
- Mair, J. L., C. J. Hart, and J. R. Stephens (2006), Deformation history of the northwestern Selwyn Basin, Yukon, Canada: Implications for orogen evolution and mid-Cretaceous magmatism, *Geological Society of America Bulletin*, 118(3-4), 304-323.
- Maloof, T. L., T. Baker, and J. F. Thompson (2001), The Dublin gulch intrusion-hosted gold deposit, Tombstone plutonic suite, Yukon territory, Canada, *Mineralium Deposita*, 36, 583-593.
- Marsh, E. E., R. J. Goldfarb, C. J. Hart, and C. A. Johnson (2003), Geology and geochemistry of the Clear Creek intrusion-related gold occurrences, Tintina Gold Province, Yukon, Canada, *Canadian Journal of Earth Sciences*, 40(5), 681-699.
- Maryono, A. (1998), Carlin-Style Sediment Hosted Gold Deposits: An Exploration opportunity, in *Beritan Ahli Geologi Indonesia* edited, p. 14.
- McPhie, J., and R. Cas (2015), Volcanic successions associated with ore deposits: Facies characteristics and ore-host relationships, in *The encyclopedia of volcanoes*, edited, pp. 865-879, Elsevier.
- Mehrabi, B., E. T. Fazel, and B. Yardley (2019), Ore geology, fluid inclusions and OS stable isotope characteristics of Shurab Sb-polymetallic vein deposit, eastern Iran, *Geochemistry*, 79(2), 307-322.





- Meinert, L. D. (1992), Skarns and skarn deposits, Geoscience Canada.
- Meinert, L. D. (1998), A review of skarns that contain gold, Mineralogical Association of Canada Short Course Series, 26, 359-414.
- Meinert, L. D., G. M. Dipple, and S. Nicolescu (2005), World skarn deposits.
- Mernagh, T. P. (2001), A fluid inclusion study of the Fosterville Mine: a turbidite-hosted gold field in the Western Lachlan Fold Belt, Victoria, Australia, *Chemical Geology*, 173(1-3), 91-106.
- Meyer, C. (1988), Ore deposits as guides to geologic history of the Earth, *Annual Review of Earth and Planetary Sciences*, Vol. 16, p. 147, 16, 147.
- Morales, M. J., R. C. F. e Silva, L. M. Lobato, S. D. Gomes, C. C. Gomes, and D. A. Banks (2016), Metal source and fluid-rock interaction in the Archean BIF-hosted Lamego gold mineralization: Microthermometric and LA-ICP-MS analyses of fluid inclusions in quartz veins, Rio das Velhas greenstone belt, Brazil, *Ore Geology Reviews*, 72, 510-531.
- Morris, H. T., and D. P. Cox (1986), Descriptive model of polymetallic replacement deposits, *Mineral deposit models: US Geological Survey Bulletin*, 1693, 99-100.
- Mountain, B., and T. M. Seward (2003), Hydrosulfide/sulfide complexes of copper (I): experimental confirmation of the stoichiometry and stability of Cu (HS) 2- to elevated temperatures, *Geochimica et Cosmochimica Acta*, 67(16), 3005-3014.
- Müller, D., and D. I. Groves (1997), Potassic igneous rocks and associated gold-copper mineralization, Springer.
- Muntean, J. L., J. S. Cline, A. C. Simon, and A. A. Longo (2011), Magmatic-hydrothermal origin of Nevada's Carlin-type gold deposits, *Nature geoscience*, 4(2), 122-127.
- Nand, A. (1989), The geochemistry of the Fosterville Goldfield, Victoria, University Of Tasmania.
- Nesbitt, B. (1996), Applications of oxygen and hydrogen isotopes to exploration for hydrothermal mineralization: *Society of Economic Geologists Newsletter* no. 27.
- Ngiamte, G., O. Okunlola, C. Suh, D. Ilouga, R. Ngatcha, N. Njamnsi, N. Afahnwie, and S. Tufion (2023), Oxygen Isotope Geochemistry as a Tool in the Exploration for BIF-hosted Iron Ore Occurrences within the Precambrian Mineral Belt of Southern Cameroon, Northwestern Margin of the Congo Craton: A Review, *Geology of Ore Deposits*, 65(6), 605-624.
- Niiranen, T. (2005), Iron Oxide-Copper-Gold Deposits in Finland: case studies from the Peräpohja schist belt and, University of Helsinki
- Norton, J. J. (1989), Gold-bearing polymetallic veins and replacement deposits, US Government Printing Office.
- Nutt, C., and A. Hofstra (2007), Bald Mountain gold mining district, Nevada: A Jurassic reduced intrusion-related gold system, *Economic Geology*, 102(6), 1129-1155.
- Ohmoto, H. (1972), Systematics of sulfur and carbon isotopes in hydrothermal ore deposits, *Economic Geology*, 67(5), 551-578.
- Ohmoto, H. (1986), Stable isotope geochemistry of ore deposits, *Reviews in Mineralogy and Geochemistry*, 16(1), 491-559.
- Orris, G., J. Bliss, J. Hammarstrom, and T. Theodore (1987), Description and grades and tonnages of gold-bearing skarns Rep. 2331-1258, US Geological Survey.
- Pal, N., and B. Mishra (2002), Alteration geochemistry and fluid inclusion characteristics of the greenstone-hosted gold deposit of Hutti, Eastern Dharwar Craton, India, *Mineralium Deposita*, 37, 722-736.
- Panteleyev, A. (1996), Epithermal Au-Ag-Cu high sulphidation (H04), Selected British Columbia mineral deposit profiles, 2, 1996-1913.
- Pereira, M. L., V. Zanon, I. Fernandes, L. Pappalardo, and F. Viveiros (2024), Hydrothermal alteration and physical and mechanical properties of rocks in a volcanic environment: A review, *Earth-Science Reviews*, 104754.
- Phillips, G., and R. Powell (2010), Formation of gold deposits: a metamorphic devolatilization model, *Journal of Metamorphic geology*, 28(6), 689-718.
- Piercey, S. J., J. G. Hinchey, and G. W. Sparkes (2023), Volcanogenic massive sulfide (VMS) deposits of the Dunnage Zone of the Newfoundland Appalachians: setting, styles, key advances, and future research, *Canadian Journal of Earth Sciences*, 60(8), 1104-1142.
- Pirajno, F. (2012), The geology and tectonic settings of China's mineral deposits, Springer Science & Business Media.
- Pokrovski, G. S., M. A. Kokh, D. Guillaume, A. Y. Borisova, P. Gisquet, J.-L. Hazemann, E. Lahera, W. Del Net, O. Proux, and D. Testemale (2015), Sulfur radical species form gold deposits on Earth, *Proceedings of the National Academy of Sciences*, 112(44), 13484-13489.





- Pollard, P. J. (2000), Evidence of a magmatic fluid and metal source for Fe oxide Cu-Au mineralization, Hydrothermal iron oxide copper-gold and related deposits: A global perspective, 1, 27-41.
- Porter, T. (2010), Current understanding of iron oxide associated-alkali altered mineralised systems: Part I—an overview, Hydrothermal iron oxide copper-gold and related deposits: a global perspective, 3, 5-32.
- Poulsen, K., and M. Hannington (1996), Volcanic-associated massive sulphide gold, Geology of Canada(8), 183-196.
- Poulsen, K. H., F. Robert, and B. Dubé (2000), Geological classification of Canadian gold deposits, Bulletin of the Geological Survey of Canada, 540, 1-106.
- Prihatmoko, S., and A. Idrus (2020), Low-sulfidation epithermal gold deposits in Java, Indonesia: Characteristics and linkage to the volcano-tectonic setting, Ore Geology Reviews, 121, 103490.
- Proffett, J. M. (2003), Geology of the Bajo de la Alumbrera porphyry copper-gold deposit, Argentina, Economic Geology, 98(8), 1535-1574.
- Radtke, A. S. (1985), Geology of the Carlin gold deposit, NevadaRep. 2330-7102, US Government Printing Office.
- Ramsay, W., F. Bierlein, D. Arne, and A. VandenBerg (1998), Turbidite-hosted gold deposits of Central Victoria, Australia: their regional setting, mineralising styles, and some genetic constraints, Ore Geology Reviews, 13(1-5), 131-151.
- Randive, K., K. Hari, M. Dora, D. Malpe, and A. Bhondwe (2014), Study of fluid inclusions: methods, techniques and applications, Geological Magazine, 29(1 and 2), 19-28.
- Rhys, D. A., P. D. Lewis, and J. V. Rowland (2020), Structural controls on ore localization in epithermal gold-silver deposits: a mineral systems approach.
- Rice, C. M., R. Harmon, and T. Shepherd (1985), Central City, Colorado; the upper part of an alkaline porphyry molybdenum system, Economic Geology, 80(7), 1769-1796.
- Richards, J. P., and A. H. Mumin (2013), Magmatic-hydrothermal processes within an evolving Earth: Iron oxide-copper-gold and porphyry Cu±Mo±Au deposits, Geology, 41(7), 767-770.
- Ridley, J. (2013), Ore deposit geology, Cambridge University Press.
- Robert, F., K. Poulsen, and B. Dubé (1997), Gold deposits and their geological classification, paper presented at Proceedings of Exploration.
- Robert, F., R. Brommecker, B. T. Bourne, P. J. Dobak, C. J. McEwan, R. R. Rowe, and X. Zhou (2007), Models and exploration methods for major gold deposit types, paper presented at Proceedings of exploration 07 Fifth Decennial International Conference on Mineral Exploration.
- Rodriguez-Mustafa, M. A., A. C. Simon, I. del Real, J. F. Thompson, L. D. Bilenker, F. Barra, I. Bindeman, and D. Cadwell (2020), A continuum from iron oxide copper-gold to iron oxide-apatite deposits: Evidence from Fe and O stable isotopes and trace element chemistry of magnetite, Economic Geology, 115(7), 1443-1459.
- Rohrlach, B. D., R. R. Loucks, and T. Porter (2005), Multi-million-year cyclic ramp-up of volatiles in a lower crustal magma reservoir trapped below the Tampakan copper-gold deposit by Mio-Pliocene crustal compression in the southern Philippines, Super porphyry copper and gold deposits: A global perspective, 2, 369-407.
- Rye, R. O. (2005), A review of the stable-isotope geochemistry of sulfate minerals in selected igneous environments and related hydrothermal systems, Chemical Geology, 215(1-4), 5-36.
- Rui-Zhong, H., S. Wen-Chao, B. Xian-Wu, T. Guang-Zhi, and A. H. Hofstra (2002), Geology and geochemistry of Carlin-type gold deposits in China, Mineralium Deposita, 37, 378-392.
- Ruggieri, G., P. Lattanzi, S. S. Luxoro, R. Dessi, M. Benvenuti, and G. Tanelli (1997), Geology, mineralogy, and fluid inclusion data of the Furtei high-sulfidation gold deposit, Sardinia, Italy, Economic Geology, 92(1), 1-19.
- Sänger-von Oepen, P., G. Friedrich, and A. Kisters (1990), Comparison between the fluid characteristics of the Rodalquilar and two neighbouring epithermal gold deposits in Spain, Mineralium Deposita, 25, S36-S41.
- Sangster, D. (1984), Felsic intrusion-associated silver-lead-zinc veins, Canadian mineral deposit types, a geological synopsis: Geological Survey of Canada Report(36), 66.
- Sawkins, F. J. (1972), Sulfide ore deposits in relation to plate tectonics, The Journal of Geology, 80(4), 377-397.
- Schirra, M., O. Laurent, T. Zwyer, T. Driesner, and C. A. Heinrich (2022), Fluid evolution at the Batu Hijau porphyry Cu-Au deposit, Indonesia: Hypogene sulfide precipitation from a single-phase aqueous magmatic fluid during chlorite-white-mica alteration, Economic Geology, 117(5), 979-1012.





- Scott, A.-M., and Y. Watanabe (1998), "Extreme boiling" model for variable salinity of the Hokko low-sulfidation epithermal Au prospect, southwestern Hokkaido, Japan, *Mineralium Deposita*, 33, 568-578.
- Seal, R. R. (2006), Sulfur isotope geochemistry of sulfide minerals, *Reviews in mineralogy and geochemistry*, 61(1), 633-677.
- Seccombe, P., J. Ju, A. Andrew, B. Gulson, and K. Mizon (1993), Nature and evolution of metamorphic fluids associated with turbidite-hosted gold deposits: Hill End goldfield, NSW, Australia, *Mineralogical Magazine*, 57(388), 423-436.
- Shanks, W. C., and R. Thurston (2012), Volcanogenic massive sulfide occurrence model, US Department of the Interior, US Geological Survey.
- Shelton, K. L., T. A. McMenamy, E. H. v. Hees, and H. Falck (2004), Deciphering the complex fluid history of a greenstone-hosted gold deposit: fluid inclusion and stable isotope studies of the Giant mine, Yellowknife, Northwest Territories, Canada, *Economic Geology*, 99(8), 1643-1663.
- Shi, K., T. Ulrich, K. Wang, X. Ma, S. Li, and R. Wang (2020), Hydrothermal evolution and ore genesis of the Laozuoshan Au skarn deposit, northeast China: Constrains from mineralogy, fluid inclusion, and O–C–S–Pb isotope geochemistry, *Ore Geology Reviews*, 127, 103879.
- Sholeh, A., E. Rastad, D. Huston, J. B. Gemmel, and R. D. Taylor (2016), The Chahnaly low-sulfidation epithermal gold deposit, western Makran volcanic arc, Southeast Iran, *Economic Geology*, 111(3), 619-639.
- Sillitoe, R. (1993), Giant and bonanza gold deposits in the epithermal environment: Assessment of potential genetic factors.
- Sillitoe, R. H. (2003), Iron oxide-copper-gold deposits: an Andean view, *Mineralium Deposita*, 38, 787-812.
- Sillitoe, R. H., M. D. Hannington, and J. F. Thompson (1996), High sulfidation deposits in the volcanogenic massive sulfide environment, *Economic geology*, 91(1), 204-212.
- Sillitoe, R. H., and J. F. Thompson (1998), Intrusion–Related Vein Gold Deposits: Types, Tectono-Magmatic Settings and Difficulties of Distinction from Orogenic Gold Deposits, *Resource Geology*, 48(4), 237-250.
- Simon, G., S. E. Kesler, and S. Chryssoulis (1999), Geochemistry and textures of gold-bearing arsenian pyrite, Twin Creeks, Nevada; implications for deposition of gold in Carlin-type deposits, *Economic Geology*, 94(3), 405-421.
- Skirrow, R. G. (2022), Iron oxide copper-gold (IOCG) deposits—A review (part 1): Settings, mineralogy, ore geochemistry and classification, *Ore Geology Reviews*, 140, 104569.
- Skirrow, R. G., J. Murr, A. Schofield, D. L. Huston, S. van der Wielen, K. Czarnota, R. Coghlan, L. M. Hight, D. Connolly, and M. Doublier (2019), Mapping iron oxide Cu-Au (IOCG) mineral potential in Australia using a knowledge-driven mineral systems-based approach, *Ore Geology Reviews*, 113, 103011.
- Soloviev, S. G., S. G. Kryazhev, S. S. Dvurechenskaya, and V. I. Uyutov (2019), Geology, mineralization, fluid inclusion, and stable isotope characteristics of the Sinyukhinskoe Cu-Au skarn deposit, Russian Altai, SW Siberia, *Ore Geology Reviews*, 112, 103039.
- Soloviev, S. G., S. G. Kryazhev, and S. S. Dvurechenskaya (2013), Geology, mineralization, stable isotope geochemistry, and fluid inclusion characteristics of the Novogodnee–Monto oxidized Au–(Cu) skarn and porphyry deposit, Polar Ural, Russia, *Mineralium Deposita*, 48(5), 603-627.
- Stefánsson, A., and T. M. Seward (2004), Gold (I) complexing in aqueous sulphide solutions to 500 C at 500 bar, *Geochimica et Cosmochimica Acta*, 68(20), 4121-4143.
- Storey, C. D., and M. Smith (2017), Metal source and tectonic setting of iron oxide-copper-gold (IOCG) deposits: Evidence from an in situ Nd isotope study of titanite from Norrbotten, Sweden, *Ore Geology Reviews*, 81, 1287-1302.
- Su, W., H. Zhang, R. Hu, X. Ge, B. Xia, Y. Chen, and C. Zhu (2012), Mineralogy and geochemistry of gold-bearing arsenian pyrite from the Shuiyindong Carlin-type gold deposit, Guizhou, China: implications for gold depositional processes, *Mineralium Deposita*, 47, 653-662.
- Tajeddin, H. A., E. Rastad, A. Yaghoubpour, S. Maghfouri, J. M. Peter, R. Goldfarb, and M. Mohajjel (2019), The Barika gold-bearing Kuroko-type volcanogenic massive sulfide (VMS) deposit, Sanandaj-Sirjan zone, Iran, *Ore Geology Reviews*, 113, 103081.
- Tan, Q.-P., Y. Xia, X. Wang, Z.-J. Xie, and D.-T. Wei (2017), Carbon-oxygen isotopes and rare earth elements as an exploration vector for Carlin-type gold deposits: A case study of the Shuiyindong gold deposit, Guizhou Province, SW China, *Journal of Asian Earth Sciences*, 148, 1-12.





- Taylor, B. E. (1987), Stable isotope geochemistry of ore-forming fluids, Mineral. Assoc. Canada, Short Course Handbook, 13, 337-445.
- Taylor, B. E. (2007), Epithermal gold deposits, Mineral Deposits of Canada: A synthesis of major deposit-types, district metallogeny, the evolution of geological provinces, and exploration methods: Geological Association of Canada, Mineral Deposits Division, Special Publication, 5, 113-139.
- Theodore, T. G. (1990), Gold-bearing skarns, US Government Printing Office.
- Thompson, J. F., and R. J. Newberry (2000), Gold deposits related to reduced granitic intrusions.
- Titley, S. R. (1982), Advances in geology of the porphyry copper deposits: Southwestern North America.
- Ulrich, T., and C. A. Heinrich (2002), Geology and alteration geochemistry of the porphyry Cu-Au deposit at Bajo de la Alumbrera, Argentina, *Economic Geology*, 97(8), 1865-1888.
- Ulrich, T., D. Günther, and C. A. Heinrich (2001), The evolution of a porphyry Cu-Au deposit, based on LA-ICP-MS analysis of fluid inclusions: Bajo de la Alumbrera, Argentina, *Economic Geology*, 96(8), 1743-1774.
- Vallance, J., L. Fontboté, M. Chiaradia, A. Markowski, S. Schmidt, and T. Vennemann (2009), Magmatic-dominated fluid evolution in the Jurassic Nambija gold skarn deposits (southeastern Ecuador), *Mineralium Deposita*, 44, 389-413.
- Vearncombe, J., and M. Zelic (2015), Structural paradigms for gold: do they help us find and mine?, *Applied Earth Science*, 124(1), 2-19.
- Wang, Y., Q. Zeng, L. Zhou, S. Chu, and Y. Guo (2016), The sources of ore-forming material in the low-sulfidation epithermal Wulaga gold deposit, NE China: Constraints from S, Pb isotopes and REE pattern, *Ore Geology Reviews*, 76, 140-151.
- Weihed, P., N. Arndt, K. Billström, J.-C. Duchesne, P. Eilu, O. Martinsson, H. Papunen, and R. Lahtinen (2005), 8: Precambrian geodynamics and ore formation: The Fennoscandian Shield, *Ore Geology Reviews*, 27(1-4), 273-322.
- White, N., M. Leake, S. McCaughey, and B. Parris (1995), Epithermal gold deposits of the southwest Pacific, *Journal of geochemical exploration*, 54(2), 87-136.
- White, N. C., and J. W. Hedenquist (1995), Epithermal gold deposits: styles, characteristics and exploration, *SEG newsletter*(23), 1-13.
- Williams, P. J., M. D. Barton, D. A. Johnson, L. Fontboté, A. De Haller, G. Mark, N. H. Oliver, and R. Marschik (2005), Iron oxide copper-gold deposits: Geology, space-time distribution, and possible modes of origin.
- Wilkinson, J. (2001), Fluid inclusions in hydrothermal ore deposits, *Lithos*, 55(1-4), 229-272.
- Wu, Y., and M. Kainan (2016), Advances in Skarn Type Gold Deposits, *International Journal of Earth Sciences and Engineering*, 1916-1921.
- Wyman, D. A., K. F. Cassidy, and P. Hollings (2016), Orogenic gold and the mineral systems approach: Resolving fact, fiction and fantasy, *Ore Geology Reviews*, 78, 322-335.
- Yan, J., Mavrogenes, J. A., Liu, S., & Coulson, I. M. (2020), Fluid properties and origins of the Lannigou Carlin-type gold deposit, SW China: Evidence from SHRIMP oxygen isotopes and LA-ICP-MS trace element compositions of hydrothermal quartz. *Journal of Geochemical Exploration*, 215, 106546.
- Zengqian, H., K. Zaw, Q. Xiaoming, Y. Qingtong, Y. Jinjie, X. Mingji, F. Deming, and Y. Xianke (2001), Origin of the Gacun volcanic-hosted massive sulfide deposit in Sichuan, China: Fluid inclusion and oxygen isotope evidence, *Economic Geology*, 96(7), 1491-1512.
- Zhang, D.-h., S.-h. Zhou, T.-f. Wan, B.-b. Xi, and J.-p. Li (2011), Depth of ore deposit formation and prognosis of deep-seated ore deposits, *Geological Bulletin of China*, 30(8), 1509-1518.
- Zheng, Y.-c., S.-h. Tian, Z.-q. Hou, Q. Fu, and D.-c. Zhu (2020), Magmatic and structural controls on the tonnage and metal associations of collision-related porphyry copper deposits in southern Tibet, *Ore Geology Reviews*, 122, 103509.
- Zhong, J., Y.-J. Chen, J. Chen, J.-P. Qi, and M.-C. Dai (2018), Geology and fluid inclusion geochemistry of the Zijinshan high-sulfidation epithermal Cu-Au deposit, Fujian Province, SE China: Implication for deep exploration targeting, *Journal of Geochemical Exploration*, 184, 49-65.
- Zoheir, B., and P. Weihed (2014), Greenstone-hosted lode-gold mineralization at Dungash mine, Eastern Desert, Egypt, *Journal of African Earth Sciences*, 99, 165-187.

